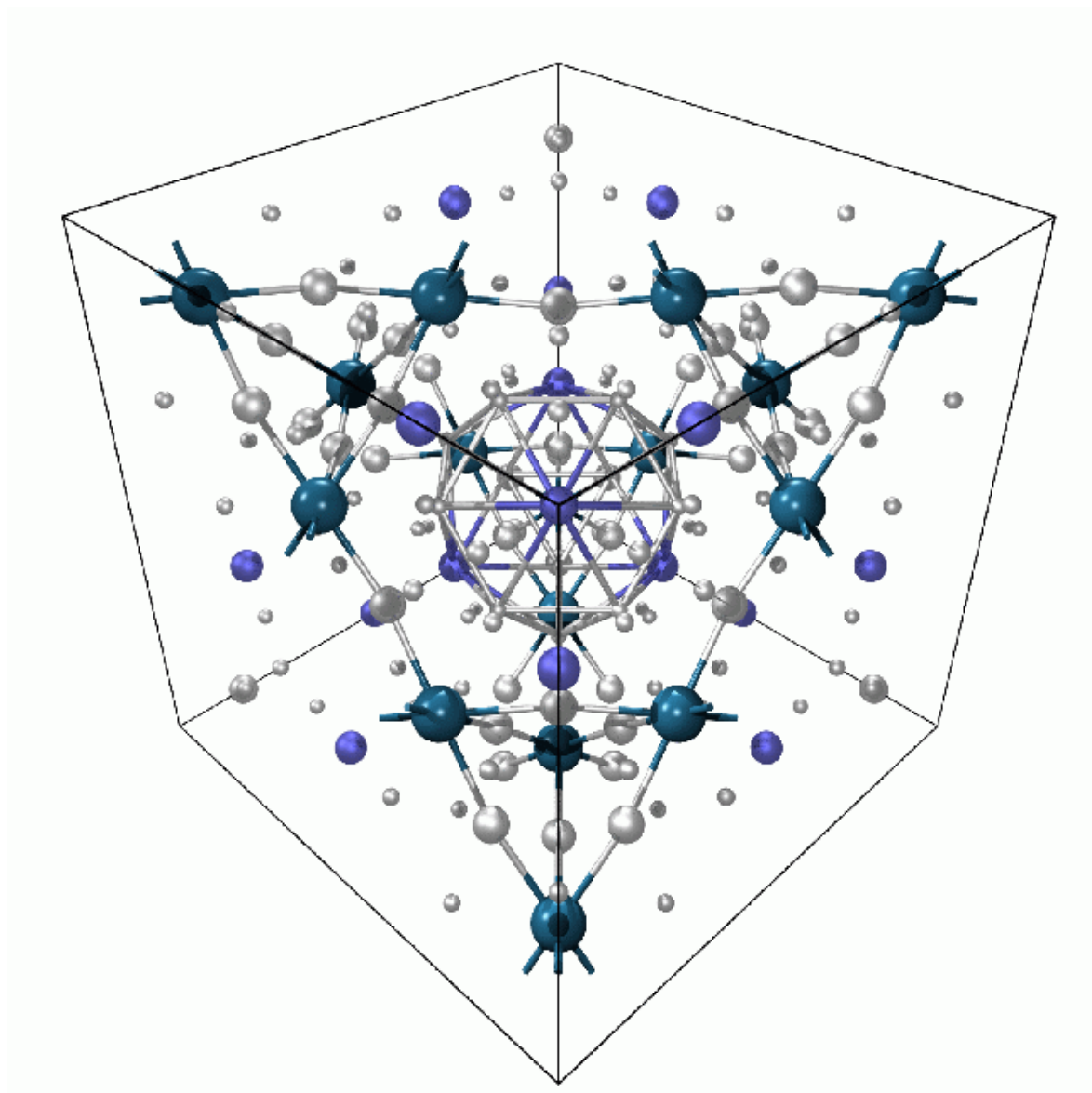


# C-MAC Days 2016



## Program and Abstracts

*Bratislava, Slovakia, November 21 -24, 2016*

# **C-MAC Days 2016**

Program and Abstracts

Editors:

Marc de Boissieu  
Marek Mihalkovič  
Peter Švec

Slovak Academy of Sciences  
and European Integrated Centre for the Development of Metallic Alloys and Compounds

Published by VEDA, Publishing House of the Slovak Academy of Sciences  
Bratislava 2016

ISBN 978-80-224-1540-8

Conference logo – Al<sub>10</sub>V crystal structure, courtesy of M. Jahňatek

# **C-MAC Days 2016**

**Bratislava, Slovakia, November 21 - 24, 2016**

## **Organizers**

C-MAC - European Integrated Centre for the Development of Metallic Alloys  
and Compounds

Institute of Physics, Slovak Academy of Sciences

Slovak University of Technology in Bratislava

Slovak Research and Development Agency

## **Co-organized by:**

Project CAVNMATT – ASFEU ITMS-26240220088

Project CEKOMAT - ASFEU ITMS-26240120020

Project KCMTE – ASFEU ITMS 26240220073

Project ENERGOZ - ASFEU ITMS 26240220028

Project VEGA 2/0189/14

Project VEGA 1/0018/15

Project APVV-15-0621

Project APVV-15-0049

Project APVV-15-0738

Project APVV-14-0934

Project APVV- 0460-12

### **General Committee**

Marc de Boissieu  
Marian Krajčí  
Marek Mihalkovič  
Peter Švec, Sr.

### **Organizing Committee**

Irena Janotová  
Peter Švec Jr.  
Peter Švec, Sr.  
Juraj Zigo  
Jozef Janovec  
Ivona Čerňáková

### **Programme Committee**

Marc de Boissieu, France  
Jozef Janovec, Slovakia  
Marian Krajčí, Slovakia  
Marek Mihalkovič, Slovakia  
Peter Švec, Sr., Slovakia

# C-MAC Days 2016

**November 21 – 24, 2016**

**Austria Trend Hotel, Bratislava, Slovakia**

## Program

### **Monday, November 21, 2016**

**16:00 - 20:00** Registration

**19:00 - 22:00** Welcome and refreshments

### **Tuesday, November 22, 2013**

**08:00 - 09:00** Registration (continued)

**08:50 - 09:00** **M. de Boissieu, M. Mihalkovic:** Welcome address

#### **Session 1:**

**09:00 - 09:30** **J. Dolinsek:** The effect of cerium on rare-earths-based hexagonal high-entropy alloys (invited lecture)

**09:30 - 09:50** **J. Cieslak:** Phase coexistence in Al<sub>x</sub>FeNiCrCo High Entropy Alloys: experimental and theoretical study

**09:50 - 10:10** **S. Vrtnik:** Magnetism of equimolar Ho-Dy-Y-Gd-Tb hexagonal HEA

**10:10 - 10:30** **Yu. Plevachuk:** Density of liquid AlCoCrCuFeNi high-entropy alloys

**10:30 - 11:00** **Coffee Break**

## **Session 2:**

**11:00 - 11:30 P. Kozelj:** Exploring superconductivity in Ta-Nb-Hf-Zr-Ti high-entropy alloys: The influence of thermal annealing (invited lecture)

**11:30 - 11:50 A. Jelen:** Complex microstructure of  $\text{CoCrFeNiZr}_x$  and  $\text{CrCuFeNi}_2\text{Al}_{1.2}$  High-Entropy Alloys explored by correlative Scanning Electron Microscope (SEM) techniques

**11:50 - 12:10 P. Gille:** Single crystal growth of  $\text{FeGa}_3$  by the Czochralski method

**12:10 - 12:30 A. Minelli:** Lattice dynamics of Monophosphate Tungsten Bronzes, quasi-2D-oxides with CDW instabilities

**12:30 - 14:00 Lunch Break**

## **Session 3:**

**14:00 - 14:30 S. Ben-Abraham:** Aperiodic tilings - an overview (invited lecture)

**14:30 - 14:50 I. Buganski:** Phason flips in the statistical approach

**14:50 - 15:10 T. Kurihara:** Composition optimization and structure refinement of Au-M-Yb (M:Si, Ga) quasicrystal approximants

**15:10 - 15:30 M. Mihalkovic:** : Unbiased prediction of quasicrystal structures from realistic atomistic simulation

**15:30 - 16:00 Coffee Break**

## **Session 4:**

**16:00 - 16:30 I. Aviziotis:** Chemical vapor deposition of Al, Fe and of the  $\text{Al}_{13}\text{Fe}_4$  approximant intermetallic phase: Experiments and multiscale simulations (invited lecture)

**16:30 - 16.50 E. Gaudry:** Structural investigation of the  $\text{Al}_5\text{Fe}_2(100)$  surface

**16:50 - 17:10 J. Janovec:** Phases of epsilon family in Al-Pd and Al-Pd-Co alloys

**17:10 - 17:30 O. Roik:** What is difference in local atomic ordering of liquid and amorphous Al-Si-Fe(Co, Ni) alloys

**17:30 - 19:00 Poster Session**

**19:00 - 21:00 Dinner**

**Wednesday, November 23, 2016**

**Session 5:**

**09:00 - 09:30 N. Mace:** Exact results on electronic wavefunctions of 2D quasicrystals (invited lecture)

**09:30 - 09:50 J. Tobola:** How electronic band structure features affect thermoelectric properties?

**09:50 - 10:10 P. Popcevic:** Magneto-transport properties of single crystal SnSe thermoelectric

**10:10 - 10:30 K. Synoradzki:** Magnetocaloric effect of  $Mn_5Ge_3$ : influence of ball milling and doping

**10:30 - 11:00 Coffee Break**

**Session 6:**

**11:00 - 11:30 R. Widmer:** Fermi states and anisotropy of Brillouin zone scattering in the decagonal Al–Ni–Co quasicrystal (invited lecture)

**11:30 - 11:50 V. Sidorov:** Crystallization of Al-Co-Dy(Ho) amorphous alloys

**11:50 - 12:10 O. Pavlosiuk:** Electronic and thermodynamic properties of rare earth-based half-Heusler compounds

**12:10 - 12:30 Yu. Grin:** Complexity of intermetallic structures: what is real and what virtual

**12:30 - 14:00 Lunch Break**

**Session 7:**

**14:00 - 14:30 P. Tomes:** Physical properties of the new rare earth clathrates  $Ba_{8-x}Eu_xAu_ySi_{46-y}$  (invited lecture)

**14:30 - 14:50 K. Anand:** Structure investigation of the (100) and (110) surfaces of the Ba-Au-Ge type-I clathrate

**14:50 - 15:10 M. de Boissieu:** Phonon lifetime and thermal conductivity in the  $Ba_{7.81}Ge_{40.67}Au_{5.33}$  clathrate

**15:10 - 15:40 Coffee Break**

**Session 8:**

**15:40 - 16:00 S. Stolz:** Asymmetric coupling reactions on the chiral PdGa{111} surfaces

- 16:00 - 16:20 M. Wencka:** Physical and catalytic properties of Ga<sub>3</sub>Ni<sub>2</sub> intermetallic - a new promising catalyst for carbon dioxide reduction
- 16:20 - 16:40 S. Coates:** Zinc Phthalocyanine (ZnPc) adsorption on Al-based intermetallic alloys
- 16:40 - 17:00 M. Krajci:** Understanding the catalytic activity of porous gold
- 17:00 - 17:10 M. de Boissieu, M. Mihalkovic:** Concluding remarks

**18:30 - 24:00 Conference Banquet**

**Thursday, November 24, 2016**

**09:00 - 10:30 Science Board Meeting**

**10:30 - 11:00 Coffee Break**

**11:00 - 12:30 Governing Board and General Assembly Meeting**

**12:30 - 14:00 Lunch**

**End of the Conference**

## List of Invited and Contributed Lectures

**I-01: S. Vrtnik, P. Koželj, J. Lužnik, Z. Jagličić, M. Feuerbacher, J. Dolinšek**

The effect of cerium on rare-earths-based hexagonal high-entropy alloys

**I-02: P. Koželj, S. Vrtnik, A. Meden, S. Maiti, W. Steurer, M. Feuerbacher, J. Dolinšek**

Exploring superconductivity in Ta-Nb-Hf-Zr-Ti high-entropy alloys: The influence of thermal annealing

**I-03: Shelomo I. Ben-Abraham**

Aperiodic tilings – an overview

**I-04: I. G. Aviziotis, T. Duguet, C. Vahlas, A. G. Boudouvis**

Chemical vapor deposition of Al, Fe and of the  $Al_{13}Fe_4$  approximant intermetallic phase: Experiments and multiscale simulations

**I-05: Nicolas Macé, Anuradha Jagannathan**

Exact results on electronic wavefunctions of 2D quasicrystals

**I-06: V. A. Rogalev, R. Widmer, O. Gröning, J. H. Dil, F. Bisti, L. L. Lev, T. Schmitt, V. N. Strocov**

Fermi states and anisotropy of Brillouin zone scattering in the decagonal Al–Ni–Co quasicrystal

**I-07: Petr Tomeš, Thomas Himmelbauer, Andrey Sidorenko, Andrey Prokofiev, Xinlin Yan, Silke Paschen**

Physical properties of the new rare earth clathrates  $Ba_{8-x}Eu_xAu_ySi_{46-y}$

**C-01: J. Cieslak, J. Tobola, K. Berent, M. Marciszko**

Phase coexistence in  $Al_xFeNiCrCo$  High Entropy Alloys: experimental and theoretical study

**C-02: S. Vrtnik, P. Koželj, J. Lužnik, A. Jelen, M. Feuerbacher, J. Dolinšek**

Magnetism of equimolar Ho-Dy-Y-Gd-Tb hexagonal HEA

**C-03: Yu. Plevachuk, J. Brillo**

Density of liquid AlCoCrCuFeNi high-entropy alloys

**C-04: Andreja Jelen, Hwanuk Guim, Janez Dolinsek**

Complex microstructure of  $CoCrFeNiZr_x$  and  $CrCuFeNi_2Al_{1.2}$  High-Entropy Alloys explored by correlative Scanning Electron Microscope (SEM) techniques

**C-05: Peter Gille, Kristian Bader, Yuri Grin**

Single crystal growth of  $FeGa_3$  by the Czochralski method

**C-06: A. Minelli, E. Duverger-Nedellec, O. Perez, A. Pautrat, M. De Boissieu, A. Bosak**

Lattice dynamics of Monophosphate Tungsten Bronzes, quasi-2D-oxides with CDW instabilities

**C-07: Ireneusz Buganski, Radoslaw Strzalka, Janusz Wolny**

Phason flips in the statistical approach

**C-08: Takuya Kurihara, Tsunetomo Yamada, An-Pang Tsai, Yurii Prots, Yuri Grin**

Composition optimization and structure refinement of Au-M-Yb (M:Si, Ga) quasicrystal approximants

**C-09: Marek Mihalkovic**

Unbiased Prediction of Quasicrystal Structures from Realistic Atomistic Simulation

**C-10: Émilie Gaudry, L. Boulley, Julian Ledieu, Marie-Cécile de Weerd, Vincent Fournée**

Structural investigation of the  $\text{Al}_5\text{Fe}_2(100)$  surface

**C-11: Jozef Janovec, Ivona Černičková, Libor Ďuriška**

Phases of epsilon family in Al-Pd and Al-Pd-Co alloys

**C-12: Oleksandr Roik, Juraj Zigo, Peter Svec**

What is difference in local atomic ordering of liquid and amorphous Al Fe(Co, Ni)-Si alloys

**C-13: K. Kutorasinski, B. Wiendlocha, S. Kaprzyk, J. Tobola**

How electronic band structure features affect thermoelectric properties?

**C-14: Petar Popčević, Marija Sorić, Peter Gille, Neven Barišić, Ana Smontara**

Magneto-transport properties of single crystal SnSe thermoelectric

**C-15: Karol Synoradzki, Tomasz Toliński**

Magnetocaloric effect of  $\text{Mn}_5\text{Ge}_3$ : influence of ball milling and doping

**C-16: V. Sidorov, S. Petrova, P. Svec Sr., P. Svec, D. Janickovic, A. Palitsina**

Crystallization of Al-Co-Dy(Ho) amorphous alloys

**C-17: O. Pavlosiuk, D. Kaczorowski, P. Wiśniewski**

Electronic and thermodynamic properties of rare earth-based half-Heusler compounds

**C-18: Yuri Gin**

Complexity of intermetallic structures: what is real and what virtual

**C-19: Kanika Anand, Émilie Gaudry, Céline Allio, Cornelius Krellner, Juri Grin, Michael Baitinger, Julian Ledieu, Vincent Fournée**

Structure investigation of the (100) and (110) surfaces of the Ba-Au-Ge type-I clathrate

**C-20: Pierre-François Lory, Stéphane Pailhès, Valentina M. Giordano, Holger Euchner, Hong Duong Nguyen, Reiner Ramlau, Horst Borrmann, Marcus Schmidt, Michael Baitinger, Matthias Ikeda, Petr Tomeš, Marek Mihalkovič, Céline Allio, Mark Robert Johnson, Helmut Schober, Yvan Sidis, Frédéric Bourdarot, Louis Pierre Regnault, Jacques Ollivier, Silke Paschen, Yuri Grin, Marc de Boissieu**

Phonon lifetime and thermal conductivity in the  $\text{Ba}_{7.81}\text{Ge}_{40.67}\text{Au}_{5.33}$  clathrate

**C-21: Samuel Stolz, Oliver Gröning, Roland Widmer**  
Asymmetric coupling reactions on the chiral PdGa{111} surfaces

**C-22: M. Wencka, P. Gille, M. Pillaca, V. Dasireddy, B. Likozar, Z. Jagličić, A. Jelen, S. Vrtnik, J. Dolinšek**  
Physical and catalytic properties of Ga<sub>3</sub>Ni<sub>2</sub> intermetallic - a new promising catalyst for carbon dioxide reduction

**C-23: Sam Coates, Abdullah Al-Mahboob, Julien Ledieu, Vincent Fournée Ronan McGrath, Hem Raj Sharma**  
Zinc Phthalocyanine (ZnPc) adsorption on Al-based intermetallic alloys

**C-24: M. Krajčí, S. Kameoka, A.-P. Tsai**  
Understanding the catalytic activity of porous gold

## List of Poster Contributions

**P-01: Alfred Amon, Lev G. Akselrud, Matej Bobnar, Maxim Avdeev, Christoph Hennig, Roman Gumeniuk, Andreas Leithe-Jasper, Yuri Grin**  
Crystal structure of a new superconducting beryllium platinum CMA

**P-02: Ivona Černičková, P. Noga, M. Adamech, Lucia Bónová, D. Vaňa, M. Muška, Anna Závacká, M. Beňo, R. Halgaš, J. Dobrovodský, J. Janovec**  
Distribution of phases in the Al-Co-Cu surface layer prepared by ion beam implantation

**P-03: M. Čulo, M. Basletić, E. Tafra, A. Hamzić, B. Korin-Hamzić**  
Spin Dependent Variable Range Hopping In Manganites  
La<sub>1-x</sub>Ca<sub>x</sub>MnO<sub>3</sub> (x > 0.5)

**P-04: Libor Ďuriška, Marián Palcut, Martin Špoták, Ivona Černičková, Ján Gondek, Pavol Priputen, Dušan Janičkovič, Jozef Janovec**  
Corrosion behaviour of selected Al-Pd alloys in aqueous NaCl

**P-05: Firas Abdel Hamid, Émilie Gaudry, M.C. De Weerd, Julian Ledieu, Vincent Fournée**  
Structure of the (100) surface of the Ce<sub>3</sub>Pd<sub>20</sub>Si<sub>6</sub> heavy fermion compound

**P-06: M. Chodyń, P. Kuczera, J. Wolny**  
Generalized Penrose Tiling as a model for structure refinement of decagonal quasicrystals

**P-07: I. Janotová, P. Švec Sr., P. Švec, I. Maťko, D. Janičkovič, J. Zigo**  
The Comparison of Rapidly quenched Co-Sn-B and Fe-Sn-B alloys

**P-08: K. Jasiewicz, B. Wiendlocha, P. Korbeń, S. Kaprzyk, J. Tobola**  
Theoretical study of electronic structure and electron-phonon coupling in Ta-Ni-Hf-Zr-Ti high entropy alloy

**P-09: Joris Kadok, Katariina Pussi, Emilie Gaudry, Marie-Cécile de Weerd, Yurii Prots, Vincent Fournee, Julian Ledieu**

Towards the formation of the  $\text{Al}_9\text{Ir}_2$  phase as surface compound

**P-10: Mirtha Pillaca, Oliver Harder, Wolfram Miller, Peter Gille**

Single crystal growth of Sb-based thermoelectric materials by *Inclined Rotary Bridgman* method

**P-11: Pavol Priputen, Marián Drienovský, Ivona Černičková, Jozef Janovec**

Study of phase equilibria in Ga-Co-Cu system at 830°C

**P-12: V. Sidorov, P. Svec**

Improving glass-forming ability of CoFeBSiNb alloys

**P-13: Katica Biljaković, G. Remenyi, I. A. Figueroa, R. Ristić, D. Pajić, A. Kuršumović, D. Starešinić, K. Zadro, E. Babić**

Electronic structure and properties of  $(\text{TiZrNbCu})_{1-x}\text{Ni}_x$  high entropy amorphous alloys

**P-14: Peter Svec, Peter Svec Sr., Jozef Hosko, Dusan Janickovic**

Formation of monophase  $\text{Fe}_{23}\text{B}_6$ -type alloy via crystallization of amorphous Fe-Ni-Nb-B system

**P-15: P. Švec, I. Mat'ko, J. Marcin, J. Kováč, G. Vlasák, D. Janičkovič, I. Škorvánek, P. Švec Sr.**

Structure And Properties of Soft-Magnetic Amorphous Bilayer Ribbons

**P-16: J. Zigo, O. Roik, P. Švec**

Phase transformations up to melting point in Al-(Fe, Co, Ni)-Si alloys

**Abstracts**

**Invited Lectures**



# The effect of cerium on rare-earths-based hexagonal high-entropy alloys

<sup>1</sup>S. Vrtnik, <sup>1</sup>P. Koželj, <sup>1</sup>J. Lužnik, <sup>2</sup>Z. Jagličić, <sup>3</sup>M. Feuerbacher, <sup>1</sup>J. Dolinšek

<sup>1</sup>*J. Stefan Institute and University of Ljubljana, Faculty of Mathematics and Physics, Jamova 39, SI-1000 Ljubljana, Slovenia*

<sup>2</sup>*Institute of Mathematics, Physics and Mechanics and University of Ljubljana, Faculty of Civil and Geodetic Engineering, Jadranska 19, SI-1000 Ljubljana, Slovenia*

<sup>3</sup>*Institut für Mikrostrukturforschung, Forschungszentrum Jülich, D-52425 Jülich, Germany*

...

Within the past several years, a new approach to alloy design with multiple principal elements in equimolar or near-equimolar ratios, termed high-entropy alloys (HEAs), has been proposed [1,2]. According to this concept, high entropy of mixing can stabilize disordered solid solution phases with simple structures like a body-centered cubic (bcc), a face-centered cubic (fcc) and a hexagonal close-packed (hcp) lattice and prevent formation of intermetallic phases during solidification. In order to achieve high entropy of mixing, the alloys must be composed typically of five or more (up to thirteen) major elements in similar concentrations, but do not contain any element whose concentration exceeds 50 at. %. HEAs with a hexagonal structure were discovered recently in the lanthanide series Gd-Tb-Y-Ho-Dy, which show a rich diagram of magnetic phases in the temperature–magnetic field phase diagram, comprising helical antiferromagnetic (AFM) phases, spontaneous and field-induced ferromagnetic (FM) phases and exotic magnetic phases with modulated long-range ordered moments [3,4]. Rare-earths (RE)-based HEAs containing light RE elements (from La to Eu) have not been investigated as yet. Mixing of light and heavy RE elements is less favorable regarding the Hume-Rothery rule of equal crystal structures. Among the light RE metals, cerium is exceptional because being at the beginning of the RE series (having one 4f electron), the spatial extent of the 4f wavefunction is the largest, so that the exchange interaction between the 4f electron and the conduction electrons is the strongest. The Ce metal and the Ce compounds consequently constitute a field of magnetism in themselves. Ce shows high solubility with all RE elements (with the presence of a miscibility gap, however). Due to its unprecedented physical properties, it is tempting to incorporate Ce into a RE-based HEA as one of the constituent elements. Since the magnetism of light RE elements remains insufficiently understood, it makes sense to incorporate Ce into a HEA composed of heavy RE elements, whose magnetism is rather well understood. In this work we present a study of magnetism of two complementary HEA systems with hexagonal crystal lattice and almost equimolar concentrations of elements: the Ce-Gd-Tb-Dy-Ho, where Ce is alloyed with four magnetic heavy RE elements Gd, Tb, Dy and Ho, and the Gd-Tb-Dy-Ho-Lu, which contains the same four heavy RE elements, but Ce is substituted by nonmagnetic Lu. Cerium greatly changes the magnetic state of the HEA by transforming the helical AFM state into a randomly disordered ferromagnet and the effective mass of the conduction electrons is increased by one order of magnitude.

## References

- [1] J.W. Yeh, S.K. Chen, S.J. Lin, et al., *Adv. Eng. Matter.* **6**, 299 (2004).
- [2] J.W. Yeh, *Ann. Chim. Sci. Mat.* **31**, 633 (2006).
- [3] M. Feuerbacher, M. Heidelmann, C. Thomas, *Mat. Res. Lett.* **3**, 1 (2014).
- [4] J. Lužnik, P. Koželj, S. Vrtnik, A. Jelen, Z. Jagličić, A. Meden, M. Feuerbacher, J. Dolinšek, *Phys. Rev. B* **92**, 224201 (2015).

# Exploring superconductivity in Ta-Nb-Hf-Zr-Ti high-entropy alloys: The influence of thermal annealing

<sup>1</sup>P. Koželj, <sup>1</sup>S. Vrtnik, <sup>2</sup>A. Meden, <sup>3</sup>S. Maiti, <sup>3</sup>W. Steurer, <sup>4</sup>M. Feuerbacher, <sup>1</sup>J. Dolinšek

<sup>1</sup>Jozef Stefan Institute and Univ. of Ljubljana, Faculty of Math. and Phys., Ljubljana, Slovenia

<sup>2</sup>Univ. of Ljubljana, Faculty of Chemistry and Chemical Technology, Ljubljana, Slovenia

<sup>3</sup>ETH Zürich, Department of Materials, Zürich, Switzerland

<sup>4</sup>Institut für Mikrostrukturforschung, Forschungszentrum Jülich, Jülich, Germany

The first observation of superconductivity in high-entropy alloys was reported by our group in 2014 [1] based on measurements on  $\text{Ta}_{34}\text{Nb}_{33}\text{Hf}_8\text{Zr}_{14}\text{Ti}_{11}$  – a type II superconductor with a critical temperature of 7.3 K and upper critical field of 8.2 T. Before the mechanism behind this superconductivity can be explained, a necessary first step is to analyze the variation of superconductive properties in the Ta-Nb-Hf-Zr-Ti system.

This contribution will present the recently-concluded investigation of four samples of Ta-Nb-Hf-Zr-Ti high-entropy alloys of different atomic concentrations (equimolar and off-equimolar), number of components (4 and 5) and subjected to different thermal treatments. An abrupt drop to zero appears in the electrical resistivity measurements of all samples, indicating that they must all contain superconductive phases. Combining with low-temperature specific heat measurements, which prove that the samples are superconductive in the entirety of their volumes, it is concluded that the presence of superconductivity in Ta-Nb-Hf-Zr-Ti alloys is a robust phenomenon and insensitive to details of the samples' structure.

Our results show that going a step further and trying to explain details of physical properties (see Figure 1) is however not possible without taking the exact micro- and nanostructure into account. In regular (non-ideal) high-entropy alloys the structure is determined by an interplay of the mixing enthalpy, which favors local atomic ordering, and mixing entropy, which favors disorder. In samples that are cooled rapidly, the entropy wins and produces a completely random solid solution. In long-time annealed samples the nanostructure orders partially through atomic diffusion and takes the form of a three-dimensional grid of short-range ordered atomic clusters rich in Zr and Hf [2]. The different transition temperatures of the clusters and the matrix can cause a double-peaked shape in the heat capacity. Generally, one can expect the nanostructure after annealing to be a sensitive function of the number of components constituting the HEA, their concentrations, the differences in the atomic radii and the annealing temperature and time. Since the nanostructure essentially governs the electronic properties, care must be taken to include the structure into discussions of HEA superconductivity.

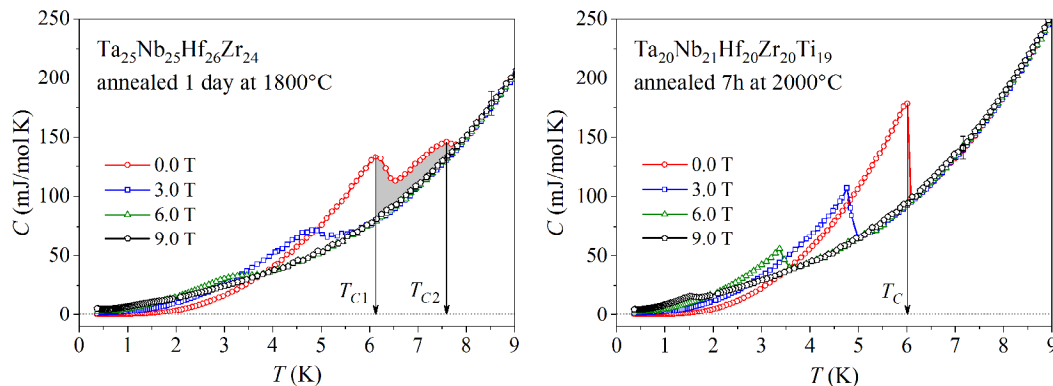


**Figure 1:** Low-temperature specific heat of differently annealed Ta-Nb-Hf-Zr-Ti samples.

[1] P. Koželj *et al.* Phys. Rev. Lett. **113**, 107001 (2014).

[2] S. Maiti, W. Steurer, Acta Mater. **106**, 87 (2016).

## **Aperiodic tilings – an overview**

Shelomo I. Ben-Abraham

*Ben-Gurion University of the Negev, Beer-Sheba, Israel*

I shall give an overview of multidimensional quasiperiodic and almost periodic (*alias* limit quasiperiodic) tilings with special emphasis on those that are being used for interpretation of real complex structures or are potential candidates for that.

I shall also deal with some more general complex tilings, such as multidimensional generalizations of non-Pisot sequences whose Fourier spectrum is singular continuous. These can serve as templates for artificial structures such as metamaterials and photonic and phononic "crystals". I shall demonstrate this on the well-known paradigmatic Prouhet-Thue-Morse structure and explicitly show how the peaks can be distinguished from Bragg peaks.

# Chemical vapor deposition of Al, Fe and of the Al<sub>13</sub>Fe<sub>4</sub> approximant intermetallic phase: Experiments and multiscale simulations

<sup>1,2</sup>I.G. Aviziotis, <sup>2</sup>T. Duguet, <sup>2</sup>C. Vahlas and <sup>1</sup>A.G. Boudouvis

<sup>1</sup>*School of Chemical Engineering, National Technical University of Athens, IroonPolytechniou 9, Zografou 157 80, Athens, Greece*

<sup>2</sup>*CIRIMAT, CNRS, Université de Toulouse, 4 allée Emile Monso, BP 44362, 31030 Toulouse cedex 4, France*

Films and coatings containing intermetallic compounds exhibit properties and combination of properties which are only partially explored today. They carry potential solutions to confer multifunctionality to advanced materials required by industrial sectors and to become a source of breakthrough and innovation. While physical vapor deposition techniques are most often used for the processing of such films and coatings, the use of metalorganic chemical vapor deposition (MOCVD) can potentially allow conformal deposition on, and functionalization of surfaces with complex geometry, with high throughput and moderate cost. The prerequisite for the implementation of such MOCVD process is the control of the complexity originating from the involved chemical reactions and transport mechanisms. In this perspective, computational modeling of the process, fed with experimental information from targeted deposition experiments, provides an integrated tool for the investigation and the understanding of the phenomena occurring at different length scales, from the macro-to the nanoscale.

MOCVD of Al-Fe intermetallic compounds is investigated in the present contribution as a paradigm of implementation of such a combined, experimental and theoretical approach. Processing of the approximant phase Al<sub>13</sub>Fe<sub>4</sub> is particularly targeted, due to its potential interest as low-cost and environmentally benign alternative to noble metal catalysts in the chemical industry<sup>1</sup>.

The processing of the targeted Al<sub>13</sub>Fe<sub>4</sub> intermetallic phase passes through the investigation of the CVD of unary Al and Fe films for the definition of the operating parameters of each deposition, to end up with a combined process, namely a co-deposition or a sequential deposition, for either the simultaneous or the successive deposition of the two metals, respectively. Through this investigation, the impact of the deposition temperatures, the operating pressures and of the mass flow rates of the initial gas mixture on the output of the CVD are experimentally and computationally examined. Furthermore, the experimentally supported computational modeling of the unary Al and Fe depositions allows fetching information concerning the chemical reactions and the microstructure of the films. This information is a valuable tool concerning the common Al and Fe processing since it reveals potential interactions in the gas phase and at the surface level. Eventually, the formation of the Al<sub>13</sub>Fe<sub>4</sub> approximant phase is achieved.

It is demonstrated that MOCVD associated with post-deposition annealing is a suitable method to obtain films composed of intermetallic alloys. Such films, conformally processed on complex surfaces can thus be considered for a variety of applications.

[1] Armbrüster, M., Konvir, K., Friedrich, M., Teschner, D., Wowsnick, G., Hahne, M., Gille, P., Szentmiklósi, L., Feuerbacher, M., Heggen, M., Girgsdies, F., Rosenthal, D., Schlögl, R., and Grin, Yu. 2012. Al<sub>13</sub>Fe<sub>4</sub> as a Low-Cost Alternative for Palladium in Heterogeneous Hydrogenation. *Nat. Mater.* 11, 690- 693.

# Exact results on electronic wavefunctions of 2D quasicrystals

Nicolas Macé, Anuradha Jagannathan

*Laboratoire de Physique des Solides, Université Paris-Sud, Orsay, France.*

Single-electron properties of 1D quasicrystals are extremely well understood: the spectrum of quasiperiodic chains can be described exactly in many situations [1], and the wavefunctions are also well characterized [2].

In contrast, even the simplest models of 2 and 3 dimensional quasicrystals resist theoretical investigations. The spectrum of a simple tight-binding model on the Penrose lattice, for instance, is only known numerically, making its physical properties still difficult to reach.

The situation changed recently, when Kalugin & Katz [3] devised from involved algebraic arguments the form of the groundstate wavefunction of generic tight-binding models on the Penrose and Ammann-Beenker tilings.

In this talk, we will show how the form of the wavefunction can be guessed from simple arguments, based on an analogy with the case of the Fibonacci chain. In a second part, we will explain how we can probe the localization degree of the groundstate on Penrose and Ammann-Beenker tilings, by computing the exact scaling of the participation ratio. Interestingly, the form of the groundstate is model-independent, meaning that we can see how the localization degree varies as we change our model – for instance by adding on-site potentials.

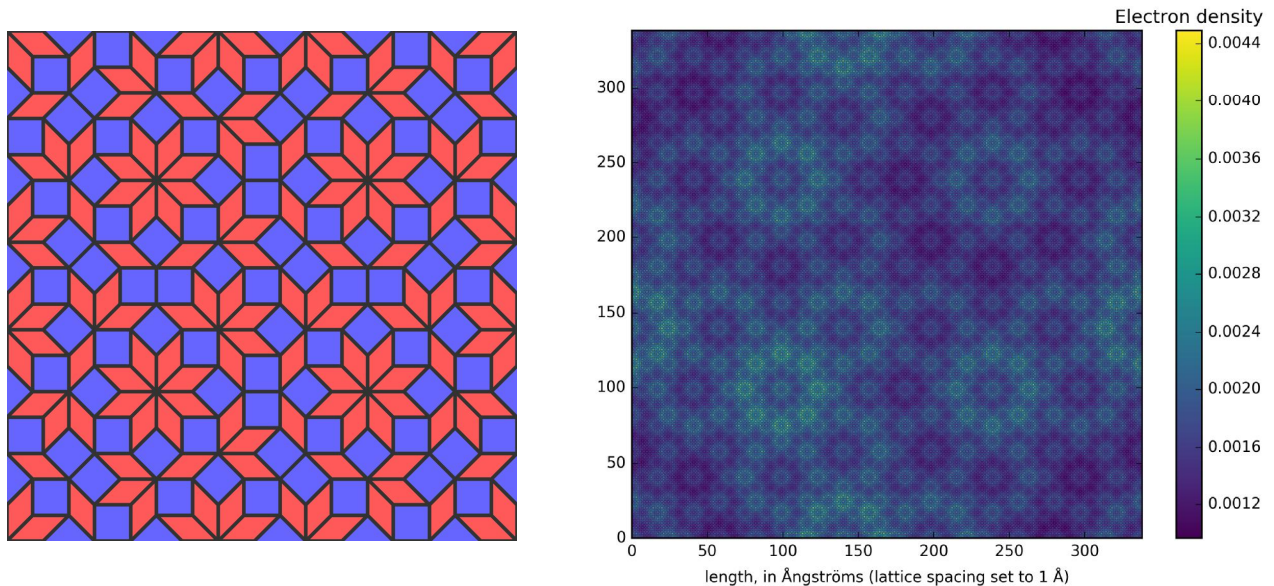


Figure: (a) A small piece of the Ammann-Beenker tiling. (b) The exact groundstate on a large piece of the Ammann-Beenker tiling (275807 sites).

[1] A. Rüdinger, C. Sire, *J Phys A*, 1996.

[2] N. Macé, A. Jagannathan, F. Piéchon, *Phys Rev B*, 2016.

[3] P. Kalugin, A. Katz, *J Phys A*, 2014.

# Fermi states and anisotropy of Brillouin zone scattering in the decagonal Al–Ni–Co quasicrystal

V.A. Rogalev<sup>1</sup>, R. Widmer<sup>2</sup>, O. Gröning<sup>2</sup>, J.H. Dil<sup>1,3</sup>, F. Bisti<sup>1</sup>, L.L. Lev<sup>1,4</sup>, T. Schmitt<sup>1</sup>, V.N. Strocov<sup>1</sup>

<sup>1</sup> Department for Synchrotron Radiation and Nanotechnology (SYN), Swiss Light Source, Paul Scherrer Institute, Villigen CH-5232, Switzerland.

<sup>2</sup> Department of Advanced Materials and Surfaces, Empa, Swiss Federal Laboratories for Materials Science and Technology, Überlandstrasse 129, 8600 Dübendorf, Switzerland.

<sup>3</sup> Institute of Condensed Matter Physics, Ecole Polytechnique Fédérale de Lausanne, 1015 Lausanne, Switzerland.

<sup>4</sup> National Research Center Kurchatov Institute, Akademika Kurchatova Square 1, 123182 Moscow, Russia.

Much effort has been devoted to understand the influence of the quasiperiodic order on the remarkable physical properties of quasicrystals (QC) [1]. The valence band electronic structure near the Fermi energy  $E_F$  in such materials is of special interest since it has a direct relation to their unusual physical properties. However, the Fermi surface (FS) topology as well as the mechanism of QC structure stabilization are still under debate. In the case of decagonal QC it is possible to directly compare properties along the quasiperiodic with those of the periodic direction. Here, we report the first observation of the three-dimensional FS and valence band dispersions near  $E_F$  in decagonal Al<sub>70</sub>Ni<sub>20</sub>Co<sub>10</sub> (d-AlNiCo) QCs using soft X-ray angle-resolved photoemission spectroscopy [2]. We show that the FS, formed by dispersive Al sp-states, has a multicomponent character due to a large contribution from high-order bands. Moreover, we discover that the magnitude of the gap at the FS related to the interaction with Brillouin zone boundary (Hume-Rothery gap) critically differs for the periodic and quasiperiodic directions.

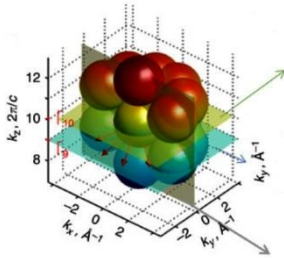


Figure 1: Sketch of the 3D FS observed in the current experiment with the planes corresponding to the different cuts at  $k_z=10(2\pi/c)$ ,  $k_z=9(2\pi/c)$  and  $k_y=0$ .

[1] Z.M. Stadnik ed., Physical Properties of Quasicrystals (Springer-Verlag, Berlin Heidelberg New York, 1999).

[2] V.A. Rogalev et al. Nature Communications 6, 8607 (2015).

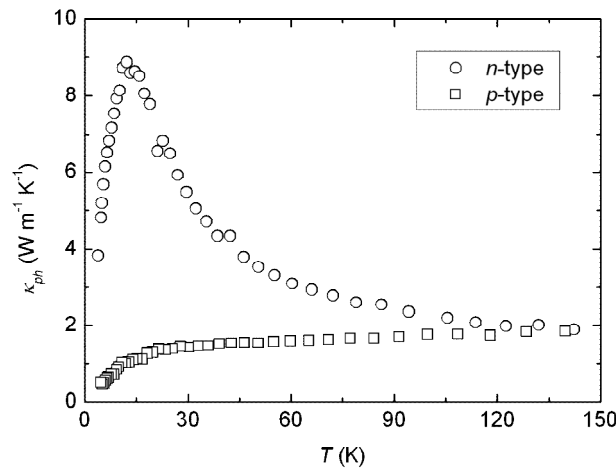
# Physical properties of the new rare earth clathrates $\text{Ba}_{8-x}\text{Eu}_x\text{Au}_y\text{Si}_{46-y}$

<sup>1</sup>Petr Tomeš, <sup>1</sup>Thomas Himmelbauer, <sup>1</sup>Andrey Sidorenko, <sup>1</sup>Andrey Prokofiev, <sup>1</sup>Xinlin Yan and <sup>1</sup>Silke Paschen

<sup>1</sup>Institute of Solid State Physics, TU Wien, Wiedner Hauptstr. 8-10, 1040 Vienna, Austria

Intermetallic clathrates have potential as thermoelectric materials for waste-heat recovery application, in particular if based on a silicon framework [1]. Substitutions with transition metal atoms add flexibility in tuning the charge carrier concentration.  $\text{Ba}_8\text{Au}_y\text{Si}_{46-y}$ , for instance, shows a metal-insulator transition as function of  $y$  [2,3]. The incorporation of some rare-earth elements into the clathrate cages leads to an enhancement of the Seebeck coefficient via electronic correlation effects [4,5]. Here, we report a study of the low-temperature transport and magnetic properties of single-crystalline  $\text{Ba}_{8-x}\text{Eu}_x\text{Au}_y\text{Si}_{46-y}$  ( $x = 1.0, 1.7$  and  $y = 4.8, 5.3$ ) type-I clathrates. Our investigations show that a transition from  $n$ - to  $p$ -type conduction takes place with increasing the Au content. The  $n$ -type sample presents a large maximum in the phonon thermal conductivity  $\kappa_{ph}$  due to the freezing of three phonon Umklapp scattering processes at low temperatures. The maximum of  $\kappa_{ph}$  in the  $p$ -type sample is strongly reduced, which we attribute to an enhanced phonon-electron coupling and to a larger Eu content. The Seebeck coefficient is well described by a diffusion term, evaluated in the free-electron approximation. Both samples are metallic and ferromagnetic, with Curie temperatures  $T_C$  of 3.1 K and 10 K for  $x = 1.0$  and 1.7, respectively, and effective magnetic moments of  $\sim 7.2 \mu_B$ , confirming the  $\text{Eu}^{2+}$  state.

We acknowledge support from the Austrian Science Fund (FWF project I623-N16).



Temperature dependence of the phonon thermal conductivities  $\kappa_{ph}(T)$  of  $\text{Ba}_{8-x}\text{Eu}_x\text{Au}_y\text{Si}_{46-y}$ .

## References:

- [1] V. L. Kuznetsov, L. A. Kuznetsovova, A. E. Kaliazin, D. M. Rowe, *J. Appl. Phys.* 87 (2000) 7871-7875.
- [2] U. Aydemir, C. Candolfi, A. Ormeci, Y. Oztan, M. Baitinger, N. Oeschler, F. Steglich, Y. Grin, *Phys. Rev. B* 84 (2011) 195137.
- [3] C. Candolfi, U. Aydemir, M. Baitinger, N. Oeschler, F. Steglich, Y. Grin, *Phys. Rev. B* 111 (2012) 043706.
- [4] A. Prokofiev, A. Sidorenko, K. Hradil, M. Ikeda, R. Svagera, M. Waas, H. Winkler, K. Neumaier, S. Paschen, *Nature Matter.* 12 (2013) 1096-1101.
- [5] S. Paschen, M. Ikeda, S. Stefanovski, G. S. Nolas, chapter 9, ed. G. S. Nolas, Series: Springer Series in Materials Science, 199 (2014) 249-276.



**Abstracts**

**Contributed Lectures**



## Phase coexistence in Al<sub>x</sub>FeNiCrCo High Entropy Alloys: experimental and theoretical study

J. Cieslak<sup>1</sup>, J. Tobola<sup>1</sup>, K. Berent<sup>2</sup> and M. Marciszko<sup>1</sup>

1. AGH University of Science and Technology, Faculty of Physics and Applied Computer Science,  
2. AGH University of Science and Technology, Academic Centre for Materials and Nanotechnology  
Al. Mickiewicza 30, 30-059 Krakow, Poland

Keywords : high entropy alloys, XRD analysis, neutron diffraction, electronic structure, crystal stability

It has already been shown that changing the contribution of only one component of HEA can result in the coexistence of two structures. This behavior occurs, for example, in the Al<sub>x</sub>FeCrNiCo HEA system, in which the transition from single *fcc* structure through the coexistence of *bcc* and *fcc* to single *bcc* structure is observed with increasing of Al content. The Korringa-Kohn-Rostoker (KKR) method with the coherent potential approximation (CPA), recently applied to calculate electronic structure, total energy and different contributions to entropy in the Al<sub>x</sub>FeCrNiCo HEA system, showed that the phase preference or phase coexistence behavior resulted from changes in the formation energy [1].

It should be however noted that for both crystalline structures observed in Al<sub>x</sub>FeCrNiCo, configuration entropies are the same, as far as their stoichiometry are maintained. If this condition is not satisfied, the configuration entropy of the system have to be reduced. In this work, the effect of the relative change in Al content with respect to other elements on observed phase coexistence/preference has been experimentally evidenced, using XRD, neutron diffraction and EDX measurements. Furthermore, electronic structure KKR and KKR-CPA calculations for two (*fcc* and *bcc*) phases with complete concentrations of elements were carried out in parallel. Obtained results well corroborate experimental data and allow to understand the reasons of the separation of particular elements between observed phases.

This work was supported by the Polish National Center of Science (NCN) under the grant UMO-2015/17/B/ST3/01204.

[1] K.Jasiewicz, J.Cieślak, S.Kaprzyk, J.Toboła, Journal of Alloys and Compounds, **648** (2015) 307-312

# Magnetism of equimolar Ho-Dy-Y-Gd-Tb hexagonal HEA

<sup>1</sup>S. Vrtnik, <sup>1</sup>P. Koželj, <sup>1</sup>J. Lužnik, <sup>1</sup>A. Jelen, <sup>2</sup>M. Feuerbacher and <sup>1</sup>J. Dolinšek

<sup>1</sup>*J. Stefan Institute and University of Ljubljana, Faculty of Mathematics and Physics,  
Jamova 39, SI-1000 Ljubljana, Slovenia*

<sup>2</sup>*Institut für Mikrostrukturforschung, Forschungszentrum Jülich, D-52425 Jülich, Germany  
E-mail: [stane.vrtnik@ijs.si](mailto:stane.vrtnik@ijs.si)*

Recently, a hexagonal HEA was synthesized using RE elements Gd, Tb, Dy, Ho and Y [1,2]. Due to zero binary mixing enthalpies of the employed elements, it is considered as an ideal HEA, stabilized by the entropy of mixing at any temperature, with random mixing of elements on the hexagonal close-packed lattice. Since these RE elements possess very disparate magnetic properties, their random mixing on an almost undistorted lattice may result in unprecedented magnetic behavior. In order to determine intrinsic magnetic properties, we have performed measurements of the magnetic and electrical response and the specific heat. The results show that the Ho-Dy-Y-Gd-Tb hexagonal HEA exhibits a rich and complex magnetic field-temperature ( $H, T$ ) phase diagram. Three characteristic temperature regions were identified between room temperature and 2 K. Within the upper temperature region, roughly between 300 and 75 K, the spin system behaves as a pure system of compositionally averaged spins, undergoing a thermodynamic phase transition to a long-range ordered helical antiferromagnetic state at the Néel temperature  $T_N = 180$  K. Region between 75 and 20 K is an intermediate region where the long-range periodic spin order “melts” and the random ordering of spins in the substitutional disorder-induced local random potential starts to prevail. Below 20 K, the spins gradually freeze in a spin glass state, which appears to be specific to the rare earths containing hexagonal HEAs.

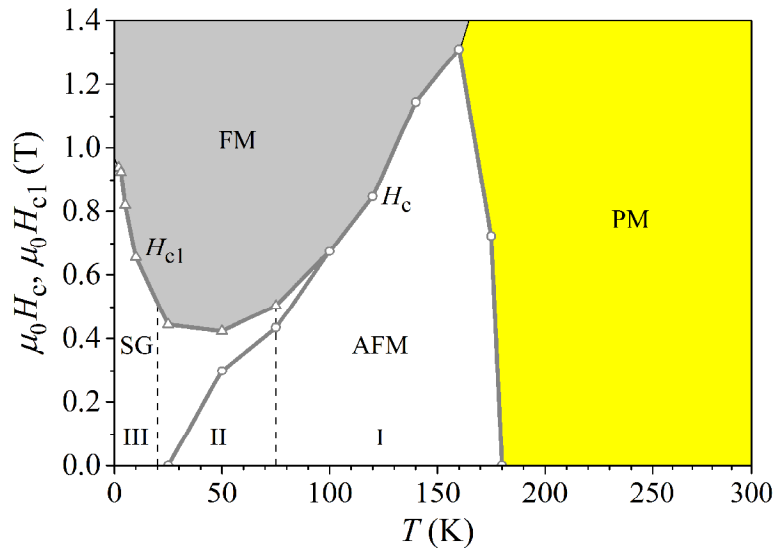


Figure 1: The ( $H, T$ ) phase diagram of equimolar Ho-Dy-Y-Gd-Tb HEA.

- [1] M. Feuerbacher, M. Heidelmann, and C. Thomas, *Mat. Res. Lett.* **3**, 1 (2014).
- [2] J. Lužnik, P. Koželj, S. Vrtnik, A. Jelen, Z. Jagličić, A. Meden, M. Feuerbacher, J. Dolinšek, *Phys. Rev. B* **92**, 224201 (2015).

## Density of liquid AlCoCrCuFeNi high-entropy alloys

<sup>1</sup> Yu. Plevachuk, <sup>2</sup> J. Brillo

<sup>1</sup> *Ivan Franko National University of Lviv, Department of Metal Physics, Lviv, Ukraine*

<sup>2</sup> *Institute of Materials Physics in Space, DLR, Cologne, Germany*

High entropy alloys (HEAs) are a novel class of metallic material with a distinct design strategy. Different from conventional alloys that are typically designed based on one or two principal elements, HEAs are composed of more than five principal elements. HEAs possess many attractive properties, such as high hardness, outstanding wear resistance, good fatigue resistance characteristics, excellent high-temperature strength, good thermal stability and, in general, good oxidation and corrosion resistance. These properties suggest great potential in a wide variety of applications. Thus, HEAs have received significant attention in recent years. Most studies on HEAs are focused on the relationships between phase, microstructure, and mechanical properties. Although less attention was paid to the physical properties of HEAs, they are actually also quite encouraging.

In this study the density of the 6-component system AlCoCrCuFeNi of equiatomic composition (16.6 at.% of each metal) and its 5- and 4-component subsystems were investigated. The density measurements were carried out with an electromagnetic levitation (EML) facility, specifically designed for optical dilatometry.

# Complex microstructure of $\text{CoCrFeNiZr}_x$ and $\text{CrCuFeNi}_2\text{Al}_{1,2}$ High-Entropy Alloys explored by correlative Scanning Electron Microscope (SEM) techniques

Andreja JELEN<sup>1,2,\*</sup>, Hwanuk GUIM<sup>2</sup>, Janez DOLINŠEK<sup>1</sup>

<sup>1</sup> Jožef Stefan Institute and Faculty of Mathematics and Physics, University of Ljubljana, Jamova 39, SI-1000 Ljubljana, Slovenia.

<sup>2</sup> Korea Basic Science Institute, Nano-Bio Electron Microscopy Research Group, 169-148 Gwahak-ro, Yuseong-gu, Daejeon 34133, Republic of Korea.

\*Postdoctoral fellow at KBSI.

High-entropy alloys (HEAs) introduce a new concept of developing advanced metallic materials with properties that conventional alloys, based on one principal element, cannot achieve [1]. They are multicomponent mixtures of 4 to 9, and occasionally up to 20 chemical elements, in similar concentrations, ranging from 5 to 35 at.% each. Though the average crystal structure of a HEA is generally simple (usually bcc or fcc), the case of microstructure might not be the same.

In our research, the HEA series of  $\text{CoCrFeNiZr}_x$  ( $x = 0.40, 0.45, \text{ and } 0.50$ ) and  $\text{CrCuFeNi}_2\text{Al}_{1,2}$  have been investigated. Various techniques, available in the state of the art SEM were employed, including high-resolution imaging, qualitative and quantitative chemical analysis and some crystallography.

The results revealed high complexity of the investigated HEAs' microstructures. An example: Fig. 1 shows FSE/BSE (forescattered/backscattered electrons) image, whereas Fig. 2 shows EBSD color-coded grains' orientations of the same area on the same sample  $\text{CoCrFeNiZr}_{0.45}$ . Correlative signals explain us many things about grain sizes and their shapes (2-D only), the type and meaning of changes in the microstructures' character, the impact of the Zr content on microstructure, etc.

[1] Y. Zhang, *et al.*, Prog. Mater. Sci. **61**, 1-93 (2014).

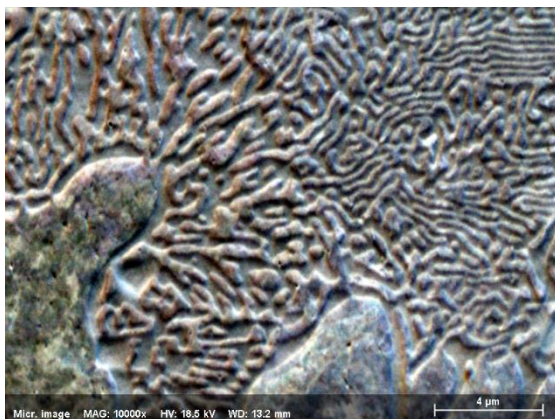


Fig. 1: FSE/BSE image of the  $\text{CoCrFeNiZr}_{0.45}$  HEA at 10.000x.

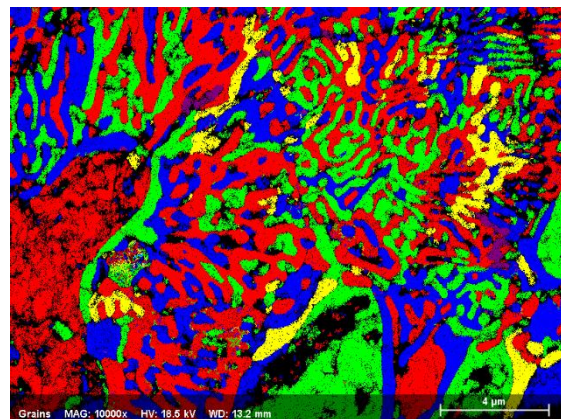


Fig. 2: Grains of the  $\text{CoCrFeNiZr}_{0.45}$  HEA at 10.000x by EBSD.

# Single crystal growth of FeGa<sub>3</sub> by the Czochralski method

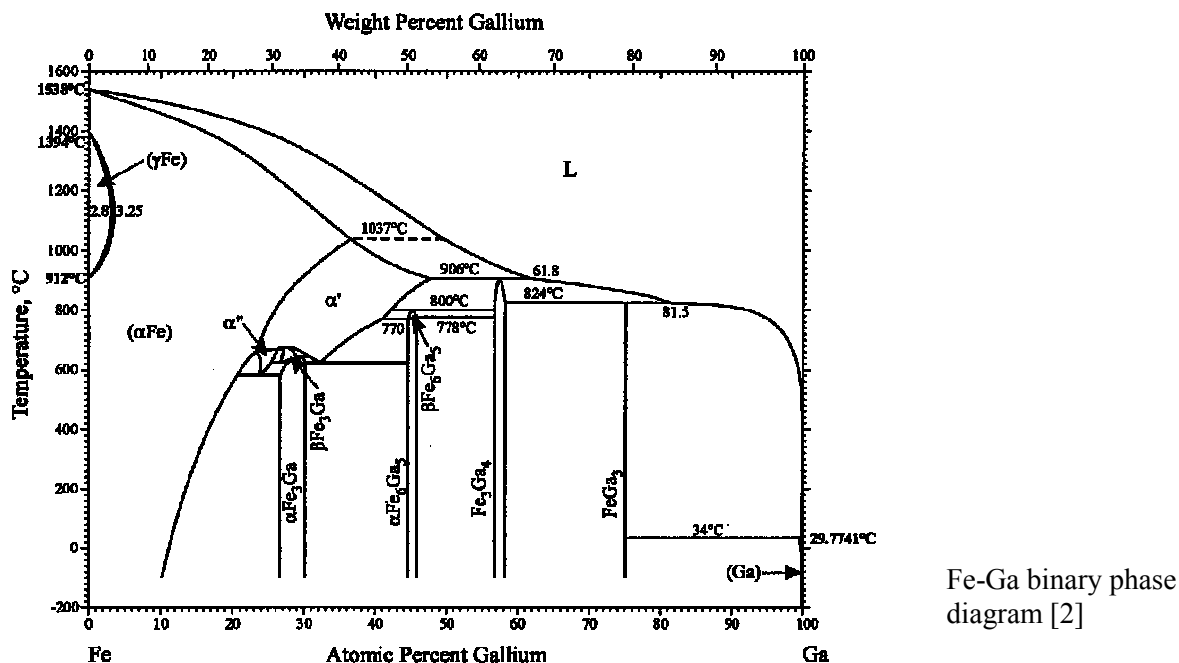
Peter Gille<sup>1</sup>, Kristian Bader<sup>1</sup>, Yuri Grin<sup>2</sup>

<sup>1</sup>Ludwig-Maximilians-Universität München, D-80333 München, Germany

<sup>2</sup>Max-Planck-Institut für Chemische Physik fester Stoffe, D-01187 Dresden, Germany

FeGa<sub>3</sub> is one of the very rare examples of semiconducting compounds that are formed from genuine metals only. This intermetallic phase, space group  $P4_2/mnm$  (No. 136), Pearson symbol  $tP16$ , is a narrow-gap semiconductor and has attracted much attention due to its interesting physical properties, e.g. with respect to thermoelectric applications [1].

According to the binary phase diagram [2], stoichiometric FeGa<sub>3</sub> peritectically decomposes at temperatures exceeding 824°C and can only be crystallized from a Ga-rich solution at temperatures lower than the peritectic one. Several single crystal growth attempts have been reported, all of them using the so-called self-flux method, i.e. spontaneous nucleation from a Ga-rich solution achieved by slow cooling a homogenized melt in a crucible. None of the authors could report on single crystals larger than a few mm in maximum dimension.



We have grown for the first time FeGa<sub>3</sub> single crystals a few cm<sup>3</sup> in size by using the Czochralski method from Ga-rich solution. Two main problems had to be solved: (i) starting the first Czochralski growth experiment without having a native seed, and (ii) finding stable growth conditions next to the peritectic temperature with a liquidus curve having an extremely unusual slope, i.e. being almost horizontal (see phase diagram). Crystal growth procedures and first results will be presented in detail.

More recent studies have suggested ferromagnetic quantum criticality in Ge-doped FeGa<sub>3</sub> with Ge substituting for Ga. Thus, we have extended our single crystal growth experiments to FeGa<sub>3-x</sub>Ge<sub>x</sub> in order to meet  $x \approx 0.15$  which is assumed to be the critical composition [3].

[1] U. Häussermann et al., J. Solid State Chem. **165**, 94 (2002).

[2] H. Okamoto, J. Phase Equil. Diff. **25**, 100 (2004).

[3] M. Majumder et al., Phys. Rev. B **93**, 064410 (2016).

## Lattice dynamics of Monophosphate Tungsten Bronzes, quasi-2D-oxides with CDW instabilities

<sup>1</sup>A. Minelli, <sup>2</sup>E. Duverger-Nedellec, <sup>2</sup>O.Perez, <sup>2</sup>A. Pautrat, <sup>3,4</sup>M. De Boissieu and <sup>1</sup>A.Bosak

<sup>1</sup> European Synchrotron Radiation Facility, 6 rue Jules Horowitz, F-38000 Grenoble, France

<sup>2</sup> Laboratory CRISMAT, UMR 6508 CNRS, ENSICAEN 6 Boulevard du Marechal Juin, F-14050 Caen Cedex 4, France

<sup>3</sup> Université Grenoble Alpes, SIMaP, F-38000 Grenoble, France

<sup>4</sup> CNRS, SIMaP, F-38000 Grenoble, France

Low-dimensional transition-metal oxides have become a subject of great interest due to their electronic instabilities, giving rise to exotic physical properties as superconductivity and charge density waves (CDW) <sup>1,2</sup>. An important subfamily of the tungsten bronzes is  $(PO_2)_4(WO_3)_{2m}$ , where the electrical/magnetic properties, band filling and anisotropies can be tuned by  $m$ , due to the different thickness in the cell of the perovskite- $WO_3$  blocks.

To understand the electronic instabilities, correlated to the nesting properties of the Fermi surface and the consequent CDW phases, the combination of two techniques, diffuse scattering (DS) and inelastic x-ray scattering (IXS), was used. The member  $P_4W_{16}O_{56}$ ,  $m=8$ , is the first we studied. It shows two different CDW transitions, at  $T_{CDW}$  260K and 145K, with different modulation vectors. Temperature-dependence DS study shows that strong modulation reflections, independent of phase, are condensed in well-defined diffuse planes, presumably defined by Fermi surface nesting properties. In figure 1, DS measurement at room temperature shows the high symmetry phase.

As we show by IXS, in high symmetry phase, those diffuse planes correspond to the valleys of soft phonons with important contribution of elastic or quasielastic scattering, which grows on cooling. Down to the CDW transition dispersion remains nearly unaffected. It seems to be the signature of an order/disorder transition, as proposed in a polaronic model by Aubry *et al.* <sup>3</sup> in the context of strong coupling theory.

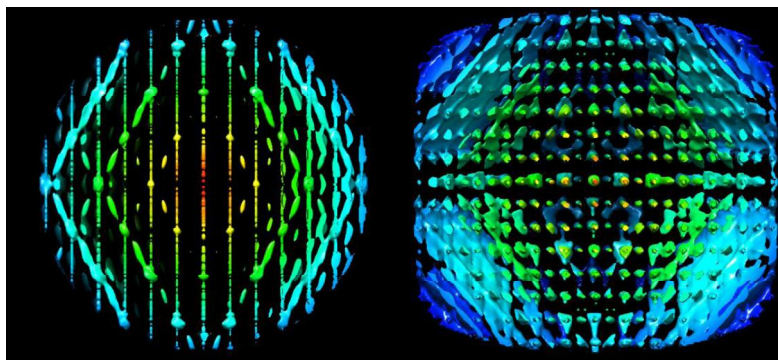


Fig.1 The 3D reconstruction of the reciprocal space taken by diffuse scattering measurements in  $P_4W_{16}O_{56}$  at room temperature (layer parallel to  $H0L$  plane – left, layer parallel to  $HK0$  plane – right).

[1] P. Fuory and J. P. Pouget, *Int. J. Mod. Phys. B* **07** (1993) 3973

[2] P. Roussel *et al.*, *Acta Cryst. B* **57** (2001) 603-632

[3] S. Aubry *et al.*, *J. Stat Phys.* **67** (1992), p. 675

# Phason flips in the statistical approach

<sup>1</sup>Ireneusz Buganski, <sup>1</sup>Radoslaw Strzalka, <sup>1</sup>Janusz Wolny

<sup>1</sup>AGH University of Science and Technology, Faculty of Physics and Applied Computer Science, Krakow, Poland

The statistical approach [1] is the alternative to commonly used higher-dimensional description of quasiperiodic structures. It takes advantage of the distribution function constructible for any type of structure. The distribution contains full structural information and allows calculating structure factor. What is more, it was recently shown that deviation from quasicrystalline order, in the form of phonons or phasons, affects the shape of the distribution in specific manner. Phasons cause discrete cuts in the distribution (Fig. 1) leading to ‘step’ like reconfiguration [2]. The final distribution function depends on the probability of the phason flip solely.

In the presentation we show how the correction of the diffraction peaks’ intensities with respect to phasons can be made within our approach apart from the general Debye-Waller correction. We postulate that improper handling of phason disorder can lead to the characteristic bias of the calculated intensities observable in all quasicrystalline models. Resignation from the phasonic Debye-Waller term in favour to the new correction can improve the quality of refined models

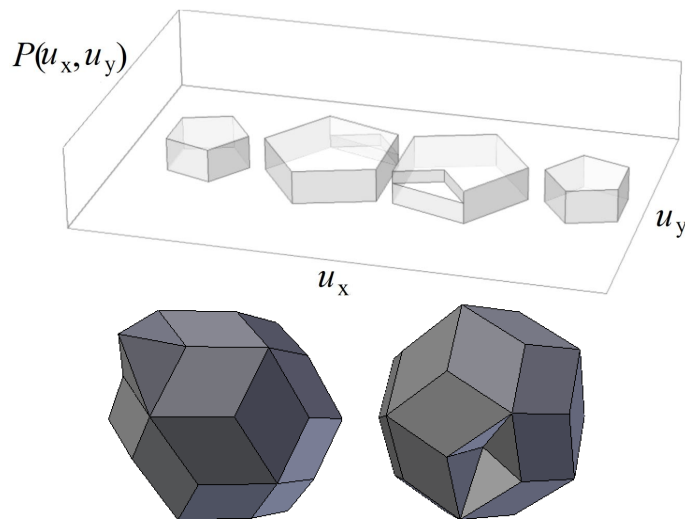


Fig. 1. Statistical distribution for vertex decoration Penrose tiling (top) and Ammann tiling (bottom) with cuts caused by phason flips.

## References

- [1] Wolny J., Philos. Mag. **A77**, 395-412, (1998).
- [2] Buganski I., Strzalka R., Wolny J., Phys. Status Solidi **B253**, 450-457, (2016).

# Composition optimization and structure refinement of Au-M-Yb (M:Si, Ga) quasicrystal approximants

<sup>1</sup>Takuya Kurihara, <sup>2</sup>Tsunetomo Yamada, <sup>2</sup>An-Pang Tsai, <sup>3</sup>Yurii Prots, <sup>3</sup>Yuri Grin

<sup>1</sup>Graduate School of Engineering, Tohoku University, Sendai, Miyagi, Japan

<sup>2</sup>IMRAM(Institute of Multidisciplinary Research for Advanced Materials), Sendai, Miyagi, Japan

<sup>3</sup>Max-Planck Institute of Chemical Physics of solids, Dresden, Germany

E-mail: [tk.takuyakurihara@gmail.com](mailto:tk.takuyakurihara@gmail.com)

Quasicrystal approximants (APs) has made the understanding of icosahedral quasicrystal (*i*-QC) deeper and more clear in the Cd - Yb system.<sup>[1]</sup> There are two similarities between APs and *i*-QC, composition and successive shell structure, so it is highly meaningful to study a composition tendency and determine a structure of APs for further perspective of *i*-QC. Various Au-M-Yb ternary APs were found by substitution of Cd with Au-M (M:other metals)<sup>[2]</sup> and the structures of Au-Si-Yb and Au-Ga-Yb 1/1 APs<sup>[3]</sup> have not been reported. Therefore we intend to identify both composition range and determine the APs structures of Au-Si-Yb and Au-Ga-Yb systems.

Each elements were arc-melted in various compositions, followed by the heat treatment using an electric furnace in Ar atmosphere. These samples were characterized by powder X-ray diffraction analysis (Cu-K $\alpha_1$ ). The crystal structure was refined by using single crystal X-ray diffraction analysis(Mo-K $\alpha$ ).

P-XRD patterns of the Au-Ga-Yb samples in various composition can be indexed with 1/1 APs of Au-Al-Yb system<sup>[4]</sup>, as shown in Figure 1(a). Although P-XRD patterns of the Au-Si-Yb samples can be also indexed in the same way, this system has narrower composition range of 1/1 APs formation (Figure 1 (b)). We will present the results of refined structures and discuss their characteristics.

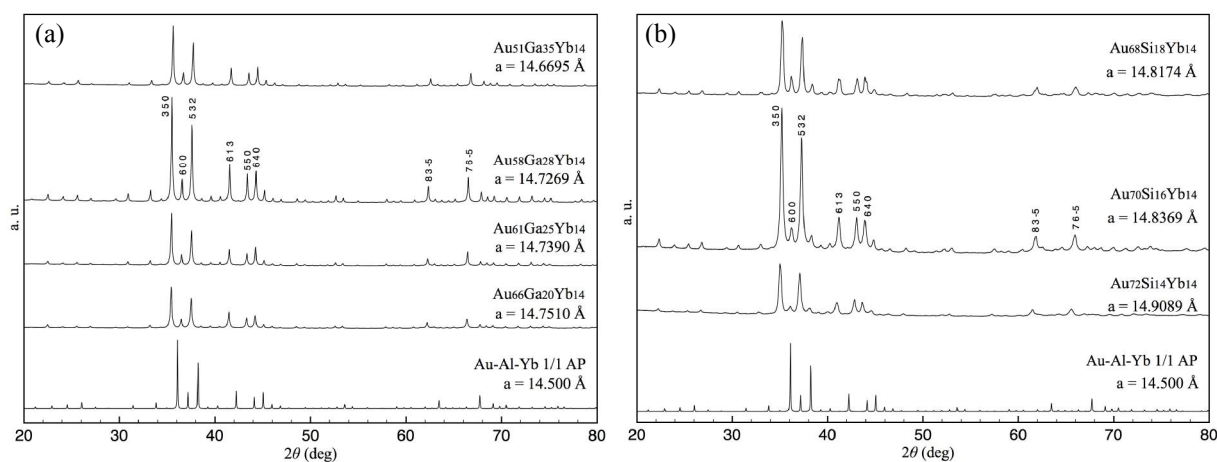


Figure 1. P-XRD patterns of (a) Au-Ga-Yb system, (b) Au-Si-Yb system

[1] Tsai, A. P., et al. "Alloys: A stable binary quasicrystal." *Nature* 408.6812 (2000): 537-538.

[2] Tsai, A. P., et al. "Approximants in the Ag-In-M and Au-Sn-M (M= Ca or Rare Earth Metals) Systems." *Japanese Journal of Applied Physics* 47.10R (2008): 7975.

[3] Watanuki, et al. "Intermediate-valence icosahedral Au-Al-Yb quasicrystal." *Physical Review B* 86.9 (2012): 094201.

[4] Ishimasa, et al. "Icosahedral quasicrystal and 1/1 cubic approximant in Au-Al-Yb alloys." *Philosophical Magazine* 91.33 (2011): 4218-4229.

# Unbiased Prediction of Quasicrystal Structures from Realistic Atomistic Simulation

Marek Mihalkovic

*Institute of Physics, Slovak Academy of Sciences, Bratislava, Slovakia*

Simulated process of melt quenching effectively suppressing diffusion barriers produces ("approximants" of) icosahedral quasicrystals in AlCuFe and AlMnPd systems by straightforward crystallization. In case of AlMnPd, the resulting low-temperature structures are unique clusters linked by  $\sim 7.6\text{\AA}$  linkages and forming so called canonical cell tiling network, in case of AlCuFe the structure exhibits variety of ever larger super clusters up to  $32\text{\AA}$  size. Ab-initio total energies of both AlCuFe and AlMnPd quasicrystal approximants are within 10 meV/atom from the tie-planes defined by the stable competing crystalline structures.

Support of the project APVV-14-0934 is acknowledged.

## Structural investigation of the $\text{Al}_5\text{Fe}_2(100)$ surface

Émilie Gaudry<sup>1</sup>, L. Boulley<sup>1</sup>, Julian Ledieu<sup>1</sup>, Marie-Cécile de Weerd<sup>1</sup>, Vincent Fournée<sup>1</sup>.

<sup>1</sup>Institut Jean Lamour, UMR 7198 CNRS-Université de Lorraine, 54011 Nancy Cedex, France.

E-mail: [emilie.gaudry@univ-lorraine.fr](mailto:emilie.gaudry@univ-lorraine.fr)

The  $\text{Al}_5\text{Fe}_2$  intermetallic compound is a good coating candidate for protecting steel from oxidation and corrosion, as an alumina former [1]. It crystallizes in the  $Cmcm$  space group with lattice parameters  $a = 7.65 \text{ \AA}$ ,  $b = 6.42 \text{ \AA}$  and  $c = 4.22 \text{ \AA}$ . The Al atoms occupy three distinct crystallographic sites: The  $\text{Al}_3$  and Fe sites form a cylindrical shape cluster structure wherein partially occupied  $\text{Al}_1$  and  $\text{Al}_2$  sites form “aluminum channels” that fill the center of the pseudo-decagonal columnar clusters [2,3] (Fig. 1).

Here we report preliminary results on the  $\text{Al}_5\text{Fe}_2(100)$  surface structure by surface science techniques under ultra-high vacuum - scanning tunneling microscopy (STM), low-energy electron diffraction (LEED), x-ray photoemission spectroscopy (XPS) - and theoretical calculations based on density functional theory (DFT). A single crystal has been grown by the Czochralski method and a sample has been extracted with a (100) orientation. A clean surface has been prepared under ultra-high vacuum conditions by repeated cycles of Ar ion sputtering and annealing. The chemical composition of the near surface region, measured by XPS as a function of the photoelectron takeoff angle, is almost constant with varying surface sensitivity. The LEED pattern indicates a  $(2 \times 2)$  surface reconstruction. Furthermore spots having a half-integer coordinate along  $c^*$  are splitted. STM images show terraces separated by a unique step height equal to twice the interlayer distance along the  $[100]$  direction ( $\approx a/2$ ). Measured 1D STM profiles along the  $[001]$  direction show maxima separated by fluctuating distances between roughly  $7.5 \text{ \AA}$  and  $9.5 \text{ \AA}$  (average value  $8.5 \text{ \AA}$ ). DFT calculations are in progress to identify the selected surface terminations in relation with the cluster substructure.

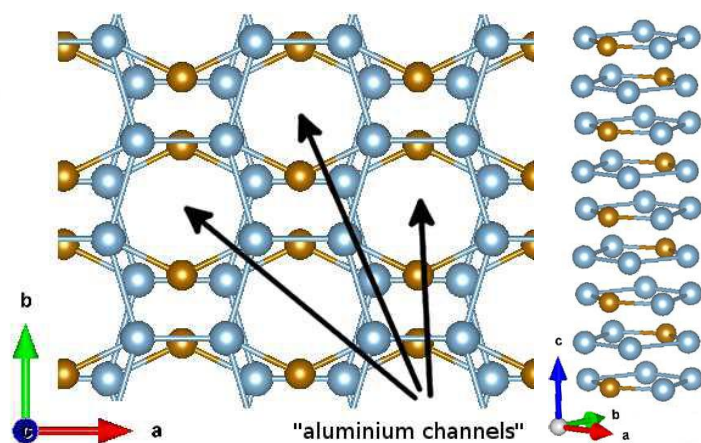


Fig.1: Cylindrical shape cluster structure of the  $\text{Al}_5\text{Fe}_2$  intermetallic compound ( $\text{Al}_3$ = blue, Fe=orange) from [2]. The “aluminum channels” are filled with  $\text{Al}_1$  and  $\text{Al}_2$  atoms (not shown).

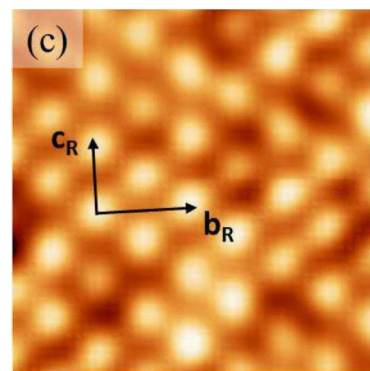


Fig.2: STM image ( $5 \times 5 \text{ nm}^2$ ,  $V_b = -2 \text{ V}$ ):  $c_R = 8.5 \text{ \AA}$  (average value) and  $b_R = 12.5 \text{ \AA}$

- [1] Sakidja et al., *Oxid. Met.* **81** (2014) 167-177
- [2] Burkhardt et al., *Acta Crystallographica* **B50** (1994) 313-316
- [3] Mihalkovic and Widom, *Phys. Rev. B* **85** (2012) 014113

## Phases of epsilon family in Al-Pd and Al-Pd-Co alloys

<sup>1</sup>Jozef Janovec, <sup>2</sup>Ivona Černičková, <sup>2</sup>Libor Ďuriška

<sup>1</sup>*Slovak University of Technology in Bratislava, Vazovova 5, 812 43 Bratislava,  
Slovak Republic*

<sup>2</sup>*Slovak University of Technology in Bratislava, Faculty of Materials Science and Technology  
in Trnava, Paulínska 16, 917 24 Trnava, Slovak Republic*

There is presented an overview of the recent results obtained by researchers at the Slovak University of Technology in Bratislava – Faculty of Materials Science and Technology in Trnava, related to both structure and properties of phases of the epsilon family in Al-Pd and Al-Pd-Co alloys. Both near-equilibrium and non-equilibrium phases were characterised using the transmission electron microscopy including electron diffraction, the scanning electron microscopy, the energy-dispersive X-ray spectroscopy, the X-ray diffraction, and the differential scanning calorimetry. The attention is paid to the description of transitions between particular types of epsilon phases. Partial changes in phase diagrams Al-Pd and Al-Pd-Co are also presented, being focussed on the area of the epsilon phase occurrence. Finally, other findings showing good potential for further investigation of epsilon phases are discussed.

### Acknowledgements

The authors wish to thank the European Regional Development Fund (ERDF) for financial support of the project ITMS:26220120014 “Center for Development and Application of Advanced Diagnostic Methods in Processing of Metallic and Non-metallic Materials” funded within the Research & Development Operational Programme, to the Grant Agency VEGA for the financial support under the contract 1/0018/15, and to the Slovak Research and Development Agency for the financial support under contracts APVV-0076-11 and APVV-15-0049.

## What is difference in local atomic ordering of liquid and amorphous Al-Fe(Co, Ni)-Si alloys

<sup>1</sup>Oleksandr Roik, <sup>2</sup>Juraj Zigo, <sup>2</sup>Peter Svec

<sup>1</sup> Taras Shevchenko National University of Kyiv, Kyiv, Ukraine

<sup>2</sup> Institute of Physics, Slovak Academy of Sciences, Bratislava, Slovakia

The rapidly solidified aluminum alloys with high Si content, which are characterized by fine and homogeneous microstructure, have already found commercial applications. However, most of amorphous Al-based alloys with Si and TM (3d-transition metal) are brittle. To improve amorphous materials knowledge about interrelationship between structure, properties and processing is required. This report presents the results of comparative analysis between the local atomic ordering in melts and the one in the amorphous alloys.

The local atomic ordering in the liquid and amorphous  $\text{Al}_{65}\text{Si}_{20}\text{Fe}_{15}$ ,  $\text{Al}_{70}\text{Si}_{20}\text{Co}_{10}$ ,  $\text{Al}_{70}\text{Si}_{20}\text{Ni}_{10}$ ,  $\text{Al}_{65}\text{Si}_{20}\text{Ni}_{15}$  alloys has been studied using X-ray scattering (Mo-K $\alpha$  radiation) and Reverse Monte Carlo simulations (RMC). The experimental total pair correlation functions,  $g(r)$ , were obtained by Fourier transform of total structure factors,  $S(Q)$ , which were calculated using coherent scattering intensity. The structure of the liquid and amorphous alloys has much in common that confirms by similarity of the  $S(Q)$  and  $g(r)$  (Fig.1). The  $S(Q)$  of both liquid and amorphous alloys have additional peak at low Q-values (prepeak) which is generally associated with presence of medium-range order and chemical short range order. However, the  $S(Q)$  of the amorphous alloys demonstrate a more pronounced prepeak in comparison with corresponding melts. The  $S(Q)$  of amorphous alloys has also shoulder on the right-hand side of the second oscillation that is usually explained by icosahedral short-range order.

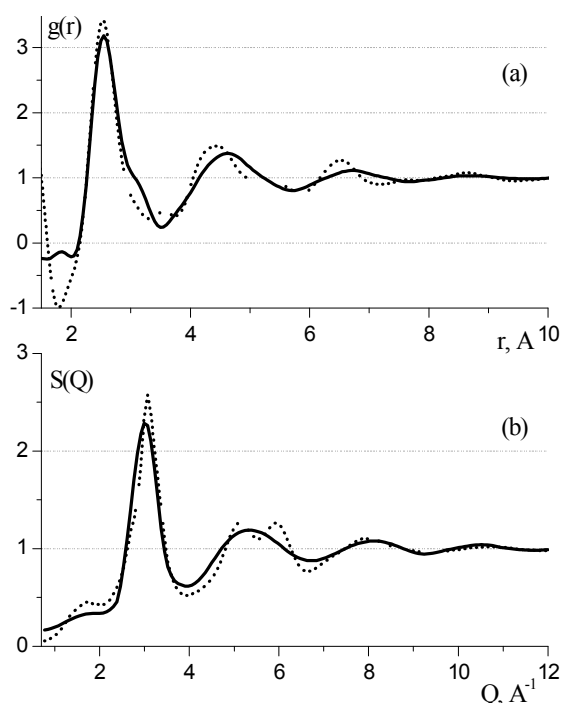


Fig.1 Structure factor (b) and pair correlation function (a) of the liquid (solid line) and amorphous (dotted)  $\text{Al}_{65}\text{Si}_{20}\text{Fe}_{15}$  alloy.

The comparison of  $g(r)$  between the liquid and amorphous alloys shows the decreasing of nearest-neighbor distance  $R_1$  (position of first peak) during glass-forming process. The maximum decreasing (from 2.57 to 2.52 Å) is observed for  $\text{Al}_{70}\text{Si}_{20}\text{Ni}_{10}$  and the minimum one (from 2.56 to 2.54 Å) for  $\text{Al}_{65}\text{Si}_{20}\text{Fe}_{15}$ . But the most prominent difference between  $g(r)$  is observed in the region of the second and third oscillations. This could indicate the small change in the first coordination sphere during the glass-formation process. There are clusters in melts with local structure that is similar to the corresponding clusters in amorphous state. However, these clusters are smaller and disordered by thermal motion. Changes in the second and third coordination sphere during the glass-formation process may point out the increasing of size of these clusters and their ordering in relation to each other.

The results of the Reverse Monte Carlo simulations of the liquid and amorphous shows that the prepeak occurs only on the partial  $S_{\text{TMTM}}(Q)$  (TM - Fe, Co or Ni) characterizing the ordering of TM atoms in relation to each other. In case of the amorphous alloys the partial  $S_{\text{TMTM}}(Q)$  demonstrate also the splitting of the second peak.

# How electronic band structure features affect thermoelectric properties?

K. Kutorasinski, B. Wiendlocha, S. Kaprzyk, J. Tobola

*Faculty of Physics and Applied Computer Science, AGH University of Science and Technology, Krakow, Poland*

Recent results electronic structure calculations, using KKR and KKR-CPA methods, as well as modeling of electron transport properties of well-known thermoelectric (TE) bulk materials are discussed. We focus mostly on the effect of electronic band convergence and the spin-orbit interaction on TE properties in  $\text{Mg}_2(\text{Si-Ge-Sn})$  on thermopower in function of carrier concentration and temperature [1] as well as on the role of the “pudding-mold-like” shape of the highest valence band (strongly nonparabolic dispersion relations) in remarkable anisotropy of electron transport properties in *p*-type orthorhombic SnSe [2]. Besides, in the case of *p*-type  $\text{Mg}_2X$  ( $X = \text{Si, Ge and Sn}$ ) series of compounds, we discuss the influence of spin-orbit interaction on TE properties, clearly evidencing that fully relativistic treatment in *ab initio* calculations may markedly affect electron transport properties [3].

This work is supported by the Polish National Science Center (NCN), under the grant Maestro DEC-2011/02/A/ST3/00124.

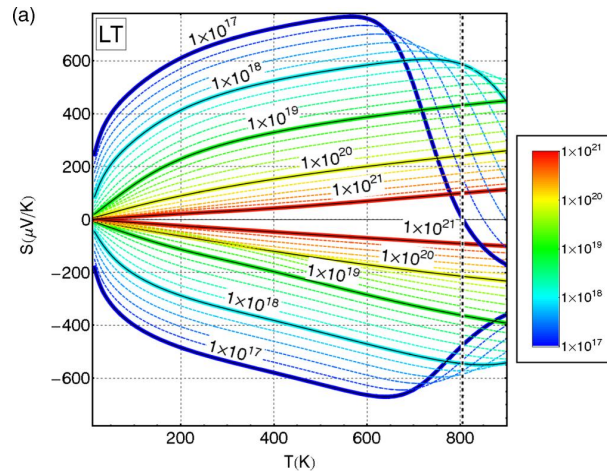


Figure: Calculated isotropic thermopower as a function of temperature for low temperature (LT) phase of SnSe upon *n*- and *p*-type doping. Different coloured lines correspond to the different carrier concentrations. Thick lines mark concentrations (in  $\text{cm}^{-3}$ ) [2].

[1] K. Kutorasinski, J. Tobola, S. Kaprzyk, *Phys. Rev. B* **87**, 195205 (2013).

[2] K. Kutorasinski, B. Wiendlocha, S. Kaprzyk, J. Tobola, *Phys. Rev. B* **91**, 205201 (2015).

[3] K. Kutorasinski, B. Wiendlocha, S. Kaprzyk, J. Tobola, *Phys. Rev. B* **89**, 115205 (2014).

## Magneto-transport properties of single crystal SnSe thermoelectric

<sup>1,2</sup>Petar Popčević, <sup>1,3</sup>Marija Sorić, <sup>4</sup>Peter Gille, <sup>2</sup>Neven Barišić, <sup>1</sup>Ana Smontara,

<sup>1</sup>*Institute of Physics, Zagreb, Croatia*

<sup>2</sup>*Institute of Solid State Physics, TU Wien, Wien, Austria*

<sup>3</sup>*Faculty of Textile Technology, University of Zagreb, Zagreb, Croatia*

<sup>4</sup>*LMU, München, Germany*

Intermetallic compound SnSe has long been known [1, 2], but its enormous thermoelectric potential was revealed just recently [3]. In this layered system, thermoelectric figure of merit  $ZT$  reaches its peak value of 2.62 at 923 K. This high  $ZT$  value is realized only in high-temperature phase that exists above 750-800 K. At room temperature, SnSe has considerably smaller  $ZT$  value. Since transition from low-temperature to high-temperature phase is displacive (shear) phase transition, several groups [4-6] have suggested that application of hydrostatic or uniaxial pressure could lower transition temperature and thus enhance  $ZT$  value in low-temperature region. In line with those theoretical predictions, recent x-ray study [6] revealed structural change at 10.5 GPa to a phase that is closely related to the high-temperature one.

As a first step in the study of this system, we have experimentally examined magneto-transport in SnSe single crystals at temperatures below room temperature. Below 70 K electrical resistivity shows negative temperature coefficient while at higher temperatures (up to at least room temperature) it exhibit  $T^2$  like behavior. In  $T^2$  regime, modified Kohler's rule was found to be valid and Seebeck coefficient shows linear behavior but with considerable residual term. At lowest temperatures where electrical resistivity exhibit NTC, Seebeck coefficient shows linear-like metallic behavior. Oscillations in Hall resistivity are observed but their periodicity changes with temperature.

- [1] J. G. Yu, *et al.*, J. Cryst. Growth **54** (1981) 248.
- [2] J. D. Wasscher, *et al.*, Solid-State Electron. **6** (1963) 261.
- [3] L.-D. Zhao, *et al.*, Nature **508** (2014) 373.
- [4] S. Alptekin, J. Mol. Model. **17** (2011) 2989.
- [5] S.M. de Suenaga, *et al.*, J. Appl. Cryst. **49** (2016) 213.
- [6] I. Loa, *et al.*, J. Phys. Condens. Matter **27** (2015) 072202.

# Magnetocaloric effect of $\text{Mn}_5\text{Ge}_3$ : influence of ball milling and doping

<sup>1,2</sup>Karol Synoradzki, <sup>2</sup>Tomasz Toliński

<sup>1</sup>*Institute of Low Temperature and Structure Research Polish Academy of Sciences, Wrocław, Poland*

<sup>2</sup>*Institute of Molecular Physics Polish Academy of Sciences, Poznań, Poland*

The intermetallic compound  $\text{Mn}_5\text{Ge}_3$  is a second-order phase transition material with Curie temperature  $T_C = 297$  K, and maximal magnetic entropy change  $\Delta S_M = 9.3 \text{ J kg}^{-1}\text{K}^{-1}$  ( $\Delta S_M/\mu_0\Delta H = 1.86 \text{ J kg}^{-1}\text{K}^{-1}\text{T}^{-1}$ ) for a field change of 5 T. This is a considerably large MCE reported in the transition metal-based compounds with second-order phase transition. The measurements of the specific heat in a wide temperature range have provided the evidence of the magnetic ordering at 297 K and the analysis of the low temperature limit of  $C_p(T)$  yields the electronic specific heat coefficient  $\gamma = 49 \text{ mJmol}^{-1}\text{K}^{-2}$  and the Debye temperature  $\Theta_D = 332$  K. Moreover,  $\text{Mn}_5\text{Ge}_3$  shows high spin polarization (up to 42%) and it grows epitaxially on Ge(111) substrates, allowing a direct injection of spin-polarized current into a semiconductor. Due to its physical properties,  $\text{Mn}_5\text{Ge}_3$  has been subjected to wide studies, including search for improving its properties by various substitutions.

Here, we demonstrate how different modifications of the  $\text{Mn}_5\text{Ge}_3$  compound affects the structural, magnetic, thermodynamic, and, especially, magnetocaloric properties. The modifications concern the granulation by ball milling and chemical substitution on Mn and Ge sites. For the case of  $\text{Mn}_5\text{Ge}_3$  the samples of different grains size were obtained by ball milling performed in a conventional horizontal ball mill. All samples crystallize in the hexagonal  $\text{Mn}_5\text{Si}_3$ -type structure with space group  $P6_3/mcm$  and order ferromagnetically. It has been also found that the ball milling process leads only to a moderate drop of the magnetocaloric effect and does not change the  $T_C$ . The reduction of the grain size by 50% decreases the refrigerant capacity (RC) by 28%. Similar effects have been observed for chemical substitutions. The replacement of Mn atoms with Co and Cr, and Ge atoms with B and Al, has reduced not only  $\Delta S_M$  and RC, but also  $T_C$ .

## Crystallization of Al-Co-Dy(Ho) amorphous alloys

<sup>1</sup>V. Sidorov, <sup>2</sup>S. Petrova, <sup>3</sup>P. Svec Sr.,  
<sup>3</sup>P. Svec, <sup>3</sup>D. Janickovic, <sup>1</sup>A. Palitsina

<sup>1</sup> *Ural State Pedagogical University, Ekaterinburg, Russia*

<sup>2</sup> *Institute of Metallurgy UD RAS, Ekaterinburg, Russia*

<sup>3</sup> *Institute of Physics SAS, Bratislava, Slovakia*

Nowadays Al-TM-REM amorphous alloys are used as protecting materials in the devices working in corrosive medium. These alloys exhibit good mechanical characteristics combining high strength and plasticity. Further improvement in the mechanical properties has been reached by partial crystallization of amorphous structures, forming a precipitation of nanometer-sized fcc-Al phase in the amorphous matrix. However, their crystallization pass depends on nature of TM (3d-transition metal) and REM (rare-earth element) and their content in the alloy.

In this work we investigated crystallization kinetics of amorphous alloys containing 8 at. % of Co and 6 or 10 at. % of Dy (Ho) by the high temperature X-ray diffraction, DSC and electrical resistivity measurements. The amorphous ribbons were prepared by the standard planar flow method in argon atmosphere. The DSC curves were obtained at heating rates of 10, 20 and 40 K/Min.

Two stages of crystallization with big heat effects were detected for Al-Co-REM alloys. It was stated that at the beginning of crystallization of  $Al_{86}Co_8R_6$  amorphous ribbons the unknown cubic phase with the lattice of Pa-3 ( $a=17,1\text{\AA}$ ) type appears. However, with the enlargement of REM content this phase disappears. The next coming phase is the  $Al_9Co_2$  compound. The both mentioned phases start to form at near  $300^0\text{ C}$  (573 K) with the difference for 10-15 degrees. Taking into account DSC results one can say that these two phases are formed at the first stage of crystallization.

The simultaneous crystallization of aluminum matrix and deposition of  $Al_3R$  compound with cubic structure take place at the second stage at near  $350^0\text{ C}$  (623 K) in  $Al_{86}Co_8R_6$  alloys.

Above  $470^0\text{ C}$  (743 K) the intermetallic compound  $Al_3R$  changes its structure from cubic to rhombohedral, and this transformation can be regarded as the third stage in crystallization. Like many other polymorphic transformations, this transition is accompanied by a small heat effect and cannot be seen on DSC curves.

It is shown, in particular, that in order to increase the stability of amorphous state it is better to use the alloy with big REM content and holmium is preferable than dysprosium.

The work is partially supported by the Ministry of Education and Science of the Russian Federation (Project no. 4.1177.2014/K).

## Electronic and thermodynamic properties of rare earth-based half-Heusler compounds

O. Pavlosiuk, D. Kaczorowski, P. Wiśniewski

*Institute of Low Temperature and Structure Research,  
Polish Academy of Sciences, Wrocław, Poland*

The compounds YPtBi, LuPtBi, HoPdBi and ErPdBi, crystallizing with a cubic MgAgAs-type crystal structure, belong to the family of half-Heusler phases intensively studied in last years. The results of *ab initio* band structure calculations showed that all these compounds have topologically non-trivial electronic structure [1-3]. We confirmed superconductivity in all these compounds by means of electrical resistivity and magnetic susceptibility measurements. The obtained critical temperatures are the following: 0.97, 0.9, 0.7, and 1.1 K for YPtBi, LuPtBi, HoPdBi and ErPdBi, respectively [4-6]. However, no clear evidence of superconducting state was revealed from the heat capacity data. We also confirmed the antiferromagnetic ordering in ErPdBi and HoPdBi at Néel temperatures 1.2 and 1.9 K, respectively [5,7].

We found features of non-trivial topology of electronic states in studied compounds. These are: non-trivial Berry phases and small effective masses extracted from the Shubnikov-de Haas oscillations observed in YPtBi, HoPdBi and ErPdBi; linear and non-saturated magnetoresistance in YPtBi and LuPtBi; weak antilocalization effect in YPtBi and HoPdBi. Moreover, propagation vectors obtained from the neutron diffraction experiments on HoPdBi and ErPdBi are  $(1/2, 1/2, 1/2)$  and conform to the theory of antiferromagnetic topological insulator [8].

Therefore, investigated compounds are prospective candidates from the point of view of coexistence of superconductivity, antiferromagnetism and non-trivial topology of electronic states.

- [1] H. Lin et al. *Nature Mat.* 9 (2010) 546.
- [2] Y. Pan et al. *Eur. Phys. Lett.* 104 (2013) 27001.
- [3] A. M. Nikitin et al. *J. Phys.: Cond. Matter* 27 (2015) 275701.
- [4] O. Pavlosiuk, D. Kaczorowski and P. Wiśniewski, *Phys. Rev. B* 94 (2016) 035130.
- [5] O. Pavlosiuk, D. Kaczorowski and P. Wiśniewski, *Sci. Rep.* 6 (2016) 18797.
- [6] O. Pavlosiuk, D. Kaczorowski and P. Wiśniewski, *Acta Phys. Pol. A* 130 (2015) 573.
- [7] O. Pavlosiuk et al. *Acta Phys. Pol. A* 127 (2015) 656.
- [8] R.S.K. Mong, A.M. Essin, and J.E. Moore, *Phys. Rev. B* 81 (2010) 245209.

# **Complexity of intermetallic structures: what is real and what virtual**

Yuri Gin

*Max-Planck-Institut für Chemische Physik fester Stoffe, Dresden, Germany*

## Structure investigation of the (100) and (110) surfaces of the Ba-Au-Ge type-I clathrate.

Kanika ANAND<sup>1</sup>, Émilie GAUDRY<sup>1</sup>, Céline ALLIO<sup>2</sup>, Cornelius KRELLNER<sup>2</sup>, Juri GRIN<sup>3</sup>,  
Michael BAITINGER<sup>3</sup>, Julian LEDIEU<sup>1</sup>, Vincent FOURNÉE<sup>1</sup>.

<sup>1</sup>Institut Jean Lamour, UMR 7198 CNRS-Université de Lorraine, 54011 Nancy Cedex, France.

<sup>2</sup>Physikalisches Institut, Goethe-Universität, Frankfurt, Frankfurt am Main, Germany.

<sup>3</sup>Max-Planck Institut für Chemische Physik fester Stoffe, Dresden, Germany.

E-mail: [vincent.fournee@univ-lorraine.fr](mailto:vincent.fournee@univ-lorraine.fr)

Clathrate and skutterudite are cage compounds and share similarities with complex metallic alloys in the sense that they are also described as a packing of highly symmetric clusters. Clathrate compounds are promising materials for thermoelectric applications, requesting low thermal and large electrical conduction to fulfil the “phonon glass – electron crystal” concept. While these compounds have been (and still are) extensively studied for their bulk properties, their surface properties remain totally unexplored.

Here we report the first study of the surface structure of the  $\text{Ba}_8\text{Au}_{5.25}\text{Ge}_{40.3}\square_{0.45}$  compound which is a type-I clathrate based on a  $sp^3$  covalently bonded polyhedral framework of Ge-Ge and Au-Ge atoms. Specifically, we would like to understand if (and how) the cage framework influences the surface structure and its properties. For this purpose, a single crystal of this phase has been grown by the Bridgman method. The  $\text{Ba}_8\text{Au}_{5.25}\text{Ge}_{40.3}\square_{0.45}$  compound has a cubic structure (space group  $Pm-3n$ ) with a lattice parameter  $a = 1.08$  nm. Its unit cell contains 54 atoms. The (100) and (110) surfaces have been both investigated by X-ray photoemission spectroscopy, low-energy electron diffraction and scanning tunneling microscopy (STM). Experimental results show no evidence for surface segregation and (1x1) bulk terminations have been observed. Unique step heights of  $0.5$  nm  $\sim a/2$  and  $0.76$  nm  $\sim a\sqrt{2}/2$  have been measured by STM for the (100) and (110) surfaces respectively, suggesting surface termination at specific planes of the bulk structure. Possible surface models have been constructed and used as input for density functional theory calculations. The surface energies of the different models have been evaluated and corresponding simulated STM images have been compared to the experimental ones. The combination of all results points towards surface terminations built by bulk truncations rather than preservations of the 3-dimensional cluster substructures.

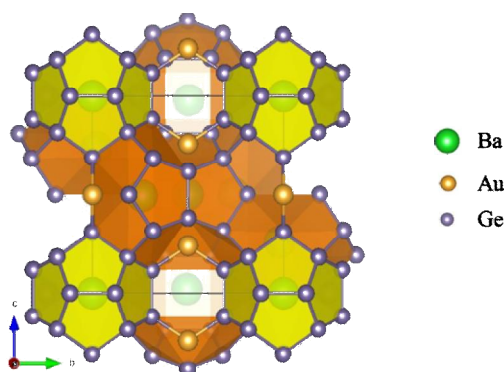


Figure: Cage-structure of the  $\text{Ba}_8\text{Au}_6\text{Ge}_{40}$  compound.

# Phonon lifetime and thermal conductivity in the $\text{Ba}_{7.81}\text{Ge}_{40.67}\text{Au}_{5.33}$ clathrate

Pierre-François Lory<sup>1,2</sup>, Stéphane Pailhès<sup>3</sup>, Valentina M. Giordano<sup>3</sup>, Holger Euchner<sup>4</sup>, Hong Duong Nguyen<sup>5</sup>, Reiner Ramlau<sup>5</sup>, Horst Borrmann<sup>5</sup>, Marcus Schmidt<sup>5</sup>, Michael Baitinger<sup>5</sup>, Matthias Ikeda<sup>7</sup>, Petr Tomeš<sup>7</sup>, Marek Mihalkovič<sup>8</sup>, Céline Allio<sup>6</sup>, Mark Robert Johnson<sup>1</sup>, Helmut Schober<sup>1-9</sup>, Yvan Sidis<sup>10</sup>, Frédéric Bourdarot<sup>11</sup>, Louis Pierre Regnault<sup>11</sup>, Jacques Ollivier<sup>1</sup>, Silke Paschen<sup>7</sup>, Yuri Grin<sup>5</sup> and Marc de Boissieu<sup>2,12</sup>

*1 Institut Laue-Langevin, 38000 Grenoble, France*

*2 Univ. Grenoble Alpes, SIMAP, 38000 Grenoble, France*

*3 Univ Lyon, University Claude Bernard Lyon 1, CNRS, Institute of Light and Matter, F-69622, Villeurbanne*

*4 Institute of Materials Science and Technology, Vienna University of Technology, 1040 Vienna, Austria*

*5 Max-Planck-Institut für Chemische Physik fester Stoffe, 01187 Dresden, Germany*

*6 Physikalisches Institut, Goethe-University, 60438 Frankfurt, Germany.*

*7 Institute of Solid State Physics, Vienna University of Technology, 1040 Vienna, Austria*

*8 Institute of Physics, Slovak Academy of Sciences, 84511 Bratislava, Slovakia*

*9 Univ. Grenoble Alpes, UFR de Physique, 38000 Grenoble, France*

*10 Laboratoire Léon Brillouin, CNRS, CEA, UMR-12, 91191 Gif sur Yvette, France*

*11 Univ. Grenoble Alpes, CEA, INAC, 38000 Grenoble, France*

*12 CNRS, SIMAP, 38000 Grenoble, France*

...

We present the direct and quantitative measurement of phonon lifetimes in a single crystal of the clathrate-I phase  $\text{Ba}_{7.81}\text{Ge}_{40.67}\text{Au}_{5.33}$ , renowned for its puzzling glass-like thermal conductivity. Surprisingly, we find that thermal transport is dominated by acoustic phonons with long lifetimes, travelling over distances from a tens to a hundred of nanometers as their wave-vectors decrease towards the center of the Brillouin zone. Considering only the three low energy acoustic phonons, and the observed energy dependence of their lifetime leads to a calculated thermal conductivity in very good agreement with the experimental one.

## Asymmetric coupling reactions on the chiral PdGa{111} surfaces

<sup>1,2</sup>Samuel Stolz, <sup>1</sup>Oliver Gröning, <sup>1</sup>Roland Widmer

<sup>1</sup>*Empa, Swiss Federal Institute for Material Science, nanotech@surface, 8600 Dübendorf, Switzerland*

<sup>2</sup>*Institute of Condensed Matter Physics, Station 3, EPFL, 1015 Lausanne, Switzerland*

Owing to the non-centrosymmetric bulk structure of the P2<sub>1</sub>3 space group PdGa exists in two enantiomeric crystal forms A and B and all surfaces of this intermetallic compound (IMC) are chiral. This fact, together with the possibility to prepare atomically flat, well-ordered surfaces in UHV, enables the investigation of asymmetric chemical surface reactions in this system.

The stacking sequence of PdGa in the [111]-direction involves four non-equivalent atomic planes, therefore the (111) and ( $\bar{1}\bar{1}\bar{1}$ ) surfaces of the same crystal form are bound to be different. Specifically, one is terminated by a single, isolated Pd atom, accordingly denoted as Pd<sub>1</sub>, while the other reveals isolated Pd trimers as the top layer, referred to as Pd<sub>3</sub> [1]. The chiral selectivity of Pd<sub>1</sub> and Pd<sub>3</sub> can be probed by adsorption of the prochiral 9-Ethynylphenanthrene (9-EP) molecule. On Pd<sub>1</sub> a huge enantiomeric excess of 94-98% is found at room temperature[2], while on Pd<sub>3</sub> a racemic mixture is observed. Post-annealing to 490 K results in the dimerization of the 9-EP on Pd<sub>1</sub>, whereas on Pd<sub>3</sub> 9-EP trimers with a homochirality of 99% are formed.

These results justify the hope to achieve highly chiral asymmetric, covalent coupling reactions. According to Nørskov *et al* the d-band center of the projected density of states (pDOS) correlates with the binding energy of a molecule and the activation energy for a reaction with another molecule [3]. Due to the copper-like d-band structure of Pd<sub>1</sub> and Pd<sub>3</sub> [1] an Azide-Alkine Huisgen Cycloaddition, which was already observed on Cu(111) under UHV conditions with similar molecules [4], is chosen as a test reaction in this regard..

For that purpose both, 9-EP and 3-(4-Azidophenyl)propionic acid, are co-adsorbed on Pd<sub>1</sub> and Pd<sub>3</sub>. After annealing to 440 K new structures are formed on Pd<sub>1</sub> which are identified as covalently coupled reaction products. The catalysed reaction is regiostereoselective on Pd<sub>1</sub> as on Cu(111), but on Pd<sub>1</sub> one out of four reaction products is favoured over the others.

No reaction, not even at temperatures as high as 600 K, between 9-EP and the acid is observed on Pd<sub>3</sub>, which leads to the conclusion that not only the d-band center, but also the surface geometry must have a big impact on its reactivity for this particular reaction [5].

### References

- [1] J. Prinz *et al*, *Angew. Chem. Int. Ed.* **51** (2012) 9339-9343
- [2] J. Prinz *et al*, *Angew. Chem.* **127** (2015) 3974-3978
- [3] J. K. Nørskov *et al*, *Nature Chemistry* **1** (2009) 37-46
- [4] F. Bebensee *et al*, *J. Am. Chem. Soc.* **135** (2013) 2136–2139
- [5] J. K. Nørskov *et al*, *Chem. Soc. Rev.* **37** (2008) 2163–2171

## Physical and catalytic properties of Ga<sub>3</sub>Ni<sub>2</sub> intermetallic - a new promising catalyst for carbon dioxide reduction

<sup>1</sup>M. Wencka, <sup>2</sup>P. Gille, <sup>2</sup>M. Pillaca, <sup>3</sup>V. Dasireddy, <sup>3</sup>B. Likozar, <sup>4</sup>Z. Jagličič,  
<sup>5</sup>A. Jelen, <sup>5</sup>S. Vrtnik, <sup>5</sup>J. Dolinšek

<sup>1</sup>*Institute of Molecular Physics, Polish Academy of Sciences, Poznań, Poland*

<sup>2</sup>*Ludwig-Maximilians-Universität München, Department of Earth and Environmental  
Sciences, Crystallography Section, München, Germany*

<sup>3</sup>*National Institute of Chemistry, Ljubljana, Slovenia*

<sup>4</sup>*Institute of Mathematics, Physics and Mechanics and University of Ljubljana, Faculty of  
Civil and Geodetic Engineering, Ljubljana, Slovenia*

<sup>5</sup>*J. Stefan Institute and University of Ljubljana, Faculty of Mathematics and Physics,  
Ljubljana, Slovenia*

Intermetallic compounds have proved to be interesting alternatives to heterogeneous catalysts prepared from pure noble metals or their alloys. Ga<sub>3</sub>Ni<sub>2</sub> is a new precious-metal-free intermetallic catalyst for CO<sub>2</sub> reduction. Other Ni-Ga compounds in a form of nanoparticles were already confirmed as catalysts for carbon dioxide reduction to methanol that is a source of green energy. Considering the Ga-Ni phase diagram, we decided to grow the only possible composition of a single crystal, namely Ga<sub>3</sub>Ni<sub>2</sub>, which allows preparing well defined surfaces for studies of its catalytic properties in heterogeneous catalysis and to determine the crystalline structure. Our cm-sized Ga<sub>3</sub>Ni<sub>2</sub> single crystal was grown from high-temperature solution using Ga as native solvent. We minimized inclusion formation of Ga-rich fluid by using an extremely low pulling rate down to 25 μm/h [1]. Ga<sub>3</sub>Ni<sub>2</sub> crystallizes in the Al<sub>3</sub>Ni<sub>2</sub>-type structure where site isolation is obvious since all Ni atoms have Ga near-neighbor environments only. For physical properties that support knowledge of the electronic and thermal contributions to the catalysis we prepared three samples cut along [100], [120] and [001] crystallographic directions. Ga<sub>3</sub>Ni<sub>2</sub> is a diamagnetic material showing magnetic susceptibility of -2 emu/g, -5 emu/g and -9 emu/g for the mentioned directions. Electrical resistivity of Ga<sub>3</sub>Ni<sub>2</sub> is metallic-type between 9 μΩcm and 11 μΩcm at 30 K, showing small anisotropy between all directions. Thermal conductivity increases rapidly in the low-temperature region up to about 50 K, whereas at higher temperatures the growth becomes slower and linear. The thermal conductivity values at 300 K are 85 W/Km for the [100] direction, 73 W/Km for the [120] direction and 53 W/Km for the [001] direction, showing the biggest anisotropy among physical properties. At 300 K, the sign of the thermoelectric power is negative only for the [120] direction and equal to -0.17 μV/K. Between 50 K and 65 K for all three directions maxima of the thermopower appear, which proves a change from non-ballistic to ballistic type of electronic transport. As the first approach toward catalysis we have tested its performance as a heterogeneous catalyst in hydrogenation reaction that reduce CO<sub>2</sub> to energy sources CO, CH<sub>4</sub> and methanol using powdered single crystal of Ga<sub>3</sub>Ni<sub>2</sub>. Ga<sub>3</sub>Ni<sub>2</sub> shows good activity towards reverse water-gas shift reaction and a high selectivity towards CO at temperatures below 400 °C.

M.W. is grateful for funding by German Academic Exchange Service (DAAD), Grant no. A/14/029042.

[1] M. Wencka, M. Pillaca, P. Gille: Single crystal growth of Ga<sub>3</sub>Ni<sub>2</sub> by Czochralski Method, Journal of Crystal Growth 449 (2016) 114-118.

## Zinc Phthalocyanine (ZnPc) adsorption on Al-based intermetallic alloys

<sup>1</sup>Sam Coates, <sup>2</sup>Abdullah Al-Mahboob, <sup>3</sup>Julien Ledieu, <sup>3</sup>Vincent Fournée <sup>1</sup>Ronan McGrath and <sup>1</sup>Hem Raj Sharma

<sup>1</sup>Surface Science Research Centre, University of Liverpool L69 3BX

<sup>2</sup>ELETTRA, Sincrotrone Trieste, 34012 Basovizza-Trieste, Italy

<sup>3</sup>Institut Jean Lamour, UMR7198 CNRS, Université de Lorraine, Nancy Cedex, France

Organic electronics are an intensely researched field of nanotechnology, with particular attention placed upon replacing expensive or inefficient in-organic materials in devices such as transistors or photovoltaics with superior organic alternatives. ZnPc is a member of a family of metal phthalocyanines (MPcs, carbon based macrocyclic compounds, with metallic centres) that have, since their discovery, have been used primarily as dyes or pigments [1]. However, MPcs are semiconductors whose properties are dependent on their crystalline structure [1] - as such, tuneable ordered molecular growth is a desirable goal for functionality.

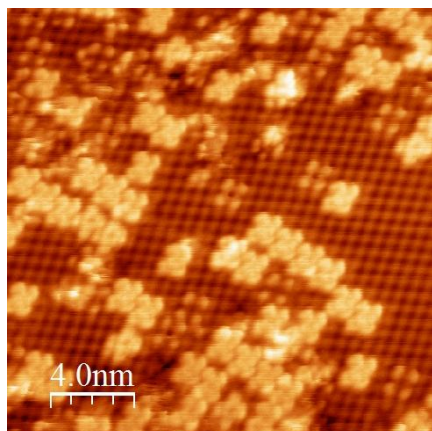


Fig. 1: STM image of low coverage of ZnPc on the Al<sub>9</sub>Co<sub>2</sub> surface

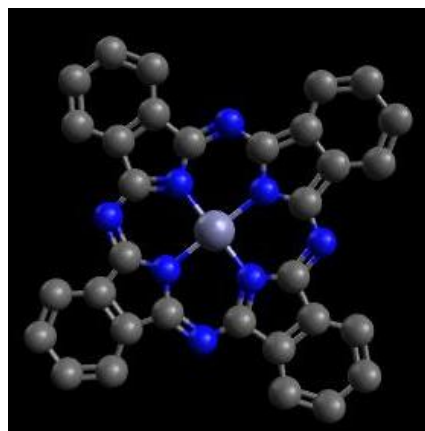


Fig. 2: ZnPc molecule

Complex metallic alloys are a fascinating area of research due to their outstanding physical properties (brittle nature, high hardness, catalytic activity etc. [2]), which indicate promising potential applications. In turn, their surfaces are of interest due to the often differing behaviour of surfaces compared to bulk behaviour, properties and structure. Here, the simple B2-NiAl and cluster based Al<sub>9</sub>Co<sub>2</sub> have been used as substrates to better understand the role that surface geometry takes in molecular adsorption and thin film growth.

Scanning Tunnelling Microscopy (STM) and Low Energy Electron Diffraction (LEED) have been used to investigate both the effect of surface complexity on adsorption behaviour and to determine any long range molecular ordering. The NiAl(100) surface presents an intriguing  $c(\sqrt{2} \times 3\sqrt{2})R45^\circ$  reconstruction which produces two unique domains. For both NiAl(100) and Al<sub>9</sub>Co<sub>2</sub>(100) there appears to be 2 preferred ZnPc adsorption sites, determined either by physical rotation due to structural complexity (NiAl) or STM brightness due to molecule-subsurface interactions (Al<sub>9</sub>Co<sub>2</sub>, Fig 1). Both results indicate promise for long-range ordered growth.

[1] M. Wojdyla *et al.*, Materials Letters, **60** (29-30), pp 3441-3446 (2006).

[2] S. A. Villaseca *et al.*, J. Phys. Chem. C, **115** (30), pp 14922-14932 (2011).

## Understanding the catalytic activity of porous gold

<sup>1</sup>M. Krajčí, <sup>2</sup>S. Kameoka, <sup>2</sup>A.-P. Tsai

<sup>1</sup>*Institute of Physics, Slovak Academy of Sciences, Bratislava 84511, Slovakia*

<sup>2</sup>*Institute of Multidisciplinary Research for Advanced Materials, Tohoku University, Sendai 980-8577, Japan*

Gold is traditionally considered as chemically inert. Contrary to most of other transition metals the surface of gold does not adsorb oxygen at ambient temperatures. Several decades ago it was discovered that if gold has a form of small ( $\approx 4$  nm) nanoparticles it becomes chemically active and can be used as catalysts for many oxidation reactions, e.g. for low-temperature CO oxidation. The catalytic activity was explained by the existence of low-coordinated atomic sites on the surface of nanoparticles, e.g. corners of the nanoparticles. A decade ago it was observed that also porous gold (PG) prepared by dealloying intermetallic compounds of Au with less noble elements as Ag, Cu, or Al also exhibits remarkable catalytic activity for oxidation reactions. The structure of PG consists of pores and ligaments with characteristic size of 30 nm - 50 nm. The observation of catalytic activity of PG was very surprising as it contradicted to the previous consensus that the characteristic size of catalytically active gold nanostructures should not exceed 5 nm. This mysterious catalytic activity of PG has not been satisfactorily explained up to now. In our recent experimental and computational study [1] we have proposed a possible explanation of this extraordinary catalytic activity of PG. In our C-MAC-Days contribution we shall present a short overview of this work.

[1] M. Krajčí, S. Kameoka, and A.-P. Tsai, *Twinning in fcc lattice creates low-coordinated catalytically active sites in porous gold*, *Journal of Chemical Physics*, **145**, 084703 (2016).

Support of the projects APVV-15-0049 and APVV-15-0621 is acknowledged.

**Abstracts**

**Poster Contributions**



# Crystal Structure of a New superconducting Beryllium Platinum CMA

<sup>1</sup> Alfred Amon, <sup>1,2</sup> Lev G. Akselrud, <sup>1</sup> Matej Bobnar, <sup>3</sup> Maxim Avdeev, <sup>4</sup> Christoph Hennig,  
<sup>5</sup> Roman Gumeniuk, <sup>1</sup> Andreas Leithe-Jasper and <sup>1</sup> Yuri Grin

<sup>1</sup> *Max-Planck Institut für Chemische Physik fester Stoffe, Nöthnitzer Str. 40, 01187 Dresden, Germany*

<sup>2</sup> *Department of Inorganic Chemistry, Ivan Franko National University of Lviv, 6 Kyryla i Mephodiya Street, Lviv 79005, Ukraine*

<sup>3</sup> *Bragg Institute, Australian Nuclear Science and Technology Organisation, Private Mail Bag 1, Menai, NSW 2234, Australia*

<sup>4</sup> *Helmholtz-Zentrum Dresden-Rossendorf, Institute of Resource Ecology, Bautzner Landstrasse 400, 01328 Dresden, Germany*

<sup>5</sup> *Tech Univ Bergakad Freiberg, Inst Expt Phys, Leipziger Str 23, D-09596 Freiberg, Germany*

Beryllium displays a diverse structural chemistry in its intermetallic compounds [1]. Electron deficiency and a high degree of covalency in beryllium-rich compounds yield interesting structural motifs where radii differences can lead to large coordination spheres.

We report on a new beryllium-rich compound in the Pt-Be system which was indexed from X-ray powder diffractometry as a face-centered cubic cell with  $a = 15.8832(2)$  Å. The crystal structure was solved with a combined effort of X-ray and neutron powder diffraction. The compound  $\text{Pt}_5\text{Be}_{21}$  constitutes a new member in the group of F-centered cubic  $\gamma$ -brass phases and can be seen as an ordered variant of the  $\text{Cu}_{41}\text{Sn}_{11}$  structure type [2,3]. The basic building blocks of the structure are 26-atom clusters which are arranged in a bcc-like pattern. Two types of cluster units are present which differ in the ordering of Pt and Be atoms on the vertices of these nested polyhedra [4]. Most interestingly, this structure type has also been observed in the Pt-Zn system, being an indication for the similar chemical behavior of Be and the group 12 transition metals [5]. Furthermore a transition into a superconducting state was observed and is currently being characterized by physical property measurements.

[1] G.V. Samsonov, *Uspekhi Khimii* 1966, **35(5)**, 779-882.

[2] A. Westgren, G. Phragmen, *Z. Anorg. Allg. Chem.* 1928, **175**, 80-89.

[3] L. Arnberg, A. Jonsson, S. Westman, *Acta Chem. Scand.* 1976, **A30(3)**, 187-192.

[4] B. Chabot, K. Cenzual, E. Parthé, *Acta Cryst.* 1981, **A37**, 6-11.

[5] S. Thimmaiah, K.W. Richter, S. Lee, B. Harbrecht, *Solid State Sci.* 2003, **5**, 1309-1317.

# Distribution of phases in the Al-Co-Cu surface layer prepared by ion beam implantation

<sup>1</sup>Ivona Černičková, <sup>1</sup>Pavol Noga, <sup>1</sup>Marek Adamech, <sup>1</sup>Lucia Bónová, <sup>1</sup>Dušan Vaňa, <sup>1</sup>Martin Muška, <sup>1</sup>Anna Závacká, <sup>1</sup>Matúš Beňo, <sup>1</sup>Radoslav Halgaš, <sup>1</sup>Jozef Dobrovodský, <sup>2</sup>Jozef Janovec

<sup>1</sup>*Slovak University of Technology in Bratislava, Faculty of Materials Science and Technology in Trnava, Paulínska 16, 917 24 Trnava, Slovak Republic*

<sup>2</sup>*Slovak University of Technology in Bratislava, Vazovova 5, 812 43 Bratislava, Slovak Republic*

The Al-based alloys can be used as coatings and/or thin films, because of their excellent surface related properties, e.g. reduced wetting with water, good oxidation resistance, low adhesion, and high hardness [1-6]. In this work, the Al-Co-Cu surface layer prepared by the ion beam implantation of Co and Cu ions into the Al substrate was studied. To obtain the structurally complex phases in the structure of surface layer, cross-sectioned samples were subsequently annealed in a vacuum furnace. In the investigation, the scanning electron microscopy including the energy-dispersive X-ray spectroscopy and the X-ray diffraction were used. Parallel, values of microhardness were measured. The distribution of phases in the microstructure was determined through the cross-section of the sample. The integrity of surface layer was established.

## References

- [1] Ledieu, J., Cox, E.J., McGrath, R. et: Step structure on the fivefold Al-Pd-Mn quasicrystal surface, and on related surface, *Surface Science* 583 (2005) 4-15
- [2] Erbudak, M., Fluckiger, T., Kortan A.R., Luscher, R.: Crystal-quasicrystal interfaces on Al-Pd-Mn, *Progress in Surface Science* 75 (2004) 161-175
- [3] Samavat, F., Gladys, M.J., et: Surface layer self-diffusion in icosahedral Al-Pd-Mn quasicrystals, *Surface Science* 601 (2007) 5678-5682
- [4] Popovic, D., Naumovic, D., Bovet, M., Koitzsch, C., Schlapbach, L., Aebi, P.: Oxidation of Al-Pd-Mn quasicrystal surfaces, *Surface Science* 492 (2001) 294-304
- [5] D.A. Rabson, Toward theories of friction and adhesion on quasicrystals, *Progress in Surface Science*, Volume 87, Issues 9–12, September–December 2012, Pages 253–271
- [6] V.N. Balbyshev, D.J. King, A.N. Khramov, L.S. Kasten, M.S. Donley, Investigation of quaternary Al-based quasicrystal thin films for corrosion protection, *Thin Solid Films*, Volumes 447–448, 30 January 2004, Pages 558–563

## Acknowledgement

The authors wish to thank the European Regional Development Fund (ERDF) for financial support of the project ITMS:26220120014 “Center for development and application of advanced diagnostic methods in processing of metallic and non-metallic materials” funded within the Research & Development Operational Programme, to the Slovak Academy of Sciences for the support in the frame of the “Center of Excellence for functional multiphase materials” (FUN-MAT, I/2/2011), as well as to the Grant Agency VEGA for the financial support under contracts 1/0018/15 and 1/0811/14, and to the Slovak Research and Development Agency for the financial support under contract APVV-15-0049.

# SPIN DEPENDENT VARIABLE RANGE HOPPING IN MANGANITES $\text{La}_{1-x}\text{Ca}_x\text{MnO}_3$ ( $x > 0.5$ )

<sup>1</sup>M. Čulo, <sup>2</sup>M. Basletić, <sup>2</sup>E. Tafra, <sup>2</sup>A. Hamzić, <sup>1</sup>B. Korin-Hamzić

<sup>1</sup>*Institute of Physics, Bijenička 46, HR-10000 Zagreb, Croatia*

<sup>2</sup>*University of Zagreb, Faculty of Science, Department of Physics, Zagreb, Croatia*

Manganites  $\text{La}_{1-x}\text{Ca}_x\text{MnO}_3$  belong to the family of manganese oxides with a general chemical formula  $R_{1-x}A_x\text{MnO}_3$ , where  $R$  represents a rare earth element or Bi and  $A$  an alkali or alkaline earth metal or Pb. Replacement of trivalent  $R$  and divalent  $A$  introduces a mixed valence state  $\text{Mn}^{3+}/\text{Mn}^{4+}$  and depending on the concentration  $x$  causes a presence of various phases in the phase diagrams of  $R_{1-x}A_x\text{MnO}_3$  [1]. A huge interest for this family of compounds started in 1994. when Jin et al. [2] found a huge decrease of resistivity in external magnetic field close to Curie temperature known as colossal magnetoresistance (CMR). CMR is present in the part of the phase diagram with ferromagnetic metallic ground state which for the investigated system  $\text{La}_{1-x}\text{Ca}_x\text{MnO}_3$  appears for concentrations  $0.2 < x < 0.5$ . Here we focused on the poorly explored part of the phase diagram  $x > 0.5$  [3] with a paramagnetic insulating phase at high, charge order phase at intermediate and antiferromagnetic insulating phase at low temperatures. We performed magnetotransport and magnetization measurements in the temperature interval 4.2-300 K and magnetic fields up to 5 T on thin film manganites for different concentrations  $0.52 \leq x \leq 0.75$ . Our results show traces of CMR and ferromagnetism and a strong coupling between magnetic and transport properties which can be interpreted in terms of spin dependent variable range hopping mechanism and a coexistence of ferromagnetic and antiferromagnetic phase.

- [1] E. Dagotto, T. Hotta, and A. Morreo, *Physics Reports* 344, 1 (2001) and references therein  
[2] S. Jin, T. H. Tiefel, M. McCormack, R. A. Fastnacht, R. Ramesh, and L. H. Chen, *Science* 264, 413 (1994)  
[3] B. Gorshunov, E. Zhukova, V. I. Torgashev, L. S. Kadyrov, E. A. Motovilova, F. Fischgrabe, V. Moshnyaga, T. Zhang, R. Kremer, U. Pracht, S. Zapf, and M. Dressel, *Phys. Rev. B* 87, 245124 (2013)

## Corrosion behaviour of selected Al-Pd alloys in aqueous NaCl

<sup>1</sup>Libor Ďuriška, <sup>1</sup>Marián Palcut, <sup>1</sup>Martin Špoták, <sup>1</sup>Ivona Černičková, <sup>1</sup>Ján Gondek, <sup>1</sup>Pavol Priputen, <sup>2</sup>Dušan Janičkovič, <sup>3</sup>Jozef Janovec

<sup>1</sup>*Slovak University of Technology in Bratislava, Faculty of Materials Science and Technology in Trnava, Paulínska 16, 917 24 Trnava, Slovak Republic*

<sup>2</sup>*Institute of Physics, Slovak Academy of Sciences, Dúbravská 9, 845 11 Bratislava, Slovak Republic*

<sup>3</sup>*Slovak University of Technology in Bratislava, Vazovova 5, 812 43 Bratislava, Slovak Republic*

The resistance to electrochemical corrosion of binary alloys with various Pd content was studied in as-cast conditions as well as after annealing at 700°C for 500 h. The alloys Al<sub>88</sub>Pd<sub>12</sub>, Al<sub>77</sub>Pd<sub>23</sub>, Al<sub>72.4</sub>Pd<sub>27.6</sub>, and Al<sub>67</sub>Pd<sub>33</sub> were prepared by arc melting of high purity Al and Pd in Ar and rapidly solidified on a water-cooled Cu mould. Structural and compositional characterizations of the alloys were done with the scanning electron microscopy coupled with the energy-dispersive X-ray spectroscopy and the X-ray diffraction. The potentiodynamic polarization of the alloys was performed in a standard 3-electrode cell in aqueous NaCl (0.6 mol.dm<sup>-3</sup>) at room temperature. To determinate corrosion potentials and corrosion current densities, Tafel extrapolation was used. The surface topography of the corroded samples was analysed using the confocal laser scanning microscopy. Phase dissolution on the alloy surfaces as well as the preferential corrosion of some of the phases was observed. The effects of phase constitution are evaluated. Results of electrochemical testing of the alloys in as-cast conditions as well as after long-term annealing are compared.

### Acknowledgements

The authors wish to thank the European Regional Development Fund (ERDF) for financial support of the project ITMS:26220120014 “Center for Development and Application of Advanced Diagnostic Methods in Processing of Metallic and Non-metallic Materials” funded within the Research & Development Operational Programme, the Grant Agency VEGA for the financial support under contracts 1/0068/14, 1/0018/15 and 1/0465/15, and the Slovak Research and Development Agency for the financial support under contracts APVV-0076-11 and APVV-15-0049.

## Structure of the (100) surface of the $\text{Ce}_3\text{Pd}_{20}\text{Si}_6$ heavy fermion compound.

Firas ABDEL HAMID<sup>1</sup>, Émilie GAUDRY<sup>1</sup>, M.C. de WEERD<sup>1</sup>, Julian LEDIEU<sup>1</sup>,  
Vincent FOURNÉE<sup>1</sup>.

<sup>1</sup>Institut Jean Lamour, UMR 7198 CNRS-Université de Lorraine, 54011 Nancy Cedex, France.

The caged compound  $\text{Ce}_3\text{Pd}_{20}\text{Si}_6$  is a complex metallic alloy crystallizing in the cubic space group  $Fm-3m$  with lattice parameter  $a = 12.16 \text{ \AA}$  [1]. Its unit cell contains 116 atoms, consisting of 12 Ce, 80 Pd and 24 Si atoms. The Ce atoms occupy two distinct crystallographic sites:  $\text{Ce}_{4a}$  are situated in cages formed by 12 Pd and 6 Si atoms while  $\text{Ce}_{8a}$  are surrounded by 16 Pd atoms (see Figure). The physical properties of this clathrate has attracted considerable attention because of heavy fermion behaviour, recent observation of quantum criticality as well as potential application for thermoelectricity [2].

Here we report preliminary results on the surface structure of this compound by scanning tunneling microscopy (STM), low-energy electron diffraction (LEED) and x-ray photoemission spectroscopy (XPS). A single crystal of this phase has been grown by the Czochralski method and a sample has been extracted with a (100) orientation. A clean surface has been prepared under ultrahigh vacuum (UHV) conditions by repeated cycles of Ar sputtering and annealing. The measured near surface composition corresponds to that of the bulk. Final state effects have been observed in the Ce  $3d$  core-levels consistent with the presence of localized Ce  $4f$  states in the valence band close to the Fermi level. A (2x2) LEED pattern is obtained after surface annealing in the range of 723 to 823 K. Two different types of terraces are observed by STM in this (2x2) regime, separated by a  $3 \text{ \AA}$  step height ( $\sim a/4$ ) (see Figure). Only one terrace type shows an STM contrast compatible with the (2x2) reconstruction, the other showing a (1x1) surface unit cell. The fractional area of the (2x2) terraces progressively decreases as the annealing temperature is increased. At 873 K and above, only the (1x1) terraces remain, partly covered with a structureless overlayer. Density functional theory (DFT) calculations are in progress to identify the selected surface terminations in relation with the cage sublattices.

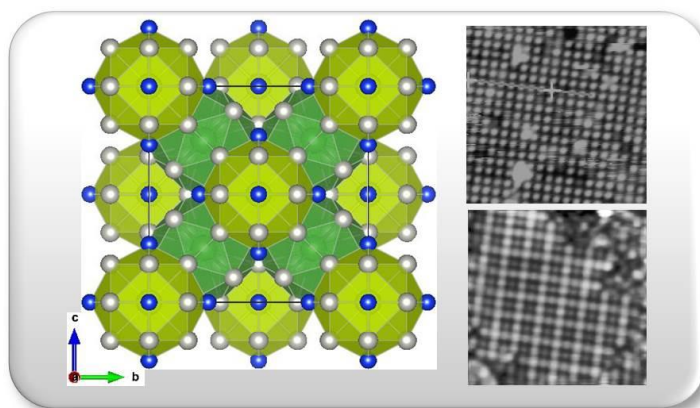


Figure : (Left) Structure model of the caged compound  $\text{Ce}_3\text{Pd}_{20}\text{Si}_6$ . (Right) STM images of the two types of terraces observed in the (2x2) regime ( $15 \times 15 \text{ nm}^2$ ).

### References:

- [1] Griбанov *et al.*, J. Alloys and Comp., 204 (1994) L9-L11.
- [2] A. Prokoviev *et al.*, Phys. Rev. B, 80 (2009) 235107.

# Generalized Penrose Tiling as a model for structure refinement of decagonal quasicrystals

M. Chodyń, P. Kuczera and J. Wolny

*Faculty of Physics and Applied Computer Science, AGH University of Science and Technology, Krakow, Poland*

The Generalized Penrose Tiling (GPT)[1,2] can be considered a promising alternative for Penrose Tiling (PT) as a model for decagonal quasicrystal refinement procedure, particularly in the statistical approach (also called the Average Unit Cell (AUC) approach) [3]. The statistical method using PT has been successfully applied to structure optimization of various decagonal phases [4]. An application of the AUC concept to the GPT[5,6] will be presented.

In the higher dimensional ( $nD$ ) approach, PT is obtained by projecting a 5D hypercubic lattice through a window consisting of four pentagons, called the atomic surfaces (ASs), in perpendicular space. The vertices of these pentagons together with two additional points form a rhombicosahedron. The GPT is created by projecting the 5D hypercubic lattice through a window consisting of five polygons, generated by shifting the ASs along the body diagonal of the rhombicosahedron. Three of the previously pentagonal ASs will become decagonal, one will remain pentagonal and one more pentagon will be created (for PT it is a single point). The structure of GPT will depend on the shift parameter. Its building units are still thick and thin rhombuses, but the matching rules and the tiling change. A diffraction pattern of GPT has peaks in the same positions as regular PT, however, their intensities are different.

First, to test possibility of refining of shift parameter, binary decagonal quasicrystal structure with arbitrary decoration for a given shift value was simulated. After successfully fitting the simulated tiling, the procedure was applied to the experimental diffraction data decagonal Al-Cu-Rh quasicrystal.

[1] K. N. Ishihara, A. Yamamoto, *Acta Cryst.* **A44**, 508-516(1988)

[2] A. Pavlovitch, M. Kleman, *J Phys a-Math Gen.* **20**, 687-702(1987)

[3] J. Wolny, *Phil. Mag.* **77**, 395-414(1998)

[4] P. Kuczera, J. Wolny, W. Steurer, *Acta Cryst.* **B68**, 578–589 (2012)

[5] B. Kozakowski, J. Wolny, *Acta Cryst.* **A66**, 489-498(2010)

[6] M. Chodyn, P. Kuczera, J. Wolny, *Acta Cryst.* **A71**, 161–168(2015)

## The Comparison of Rapidly quenched Co-Sn-B and Fe-Sn-B alloys

I. Janotová, P. Švec Sr., P. Švec, I. Maňko, D. Janičkovič, J. Zigo

*Institute of Physics, Slovak Academy of Sciences, Bratislava, Slovakia*

The metastable Fe-B, Co-B and Fe-Co-B alloys are frequently studied and commonly used as a base for different soft magnetic metallic glasses [1-5]. To improve the nanocrystallization of these systems the rare-earth elements are often used. To eliminate the need of these expensive and strategic elements the alloying by the post-transition metals could offer an alternative solution. Therefore, the addition of small amounts of Sn into the Fe-B, Co-B and Fe-Co-B based metastable systems [2-7] was studied. The difference of the atomic radii of Fe and/or Co and Sn atoms are favorable for the incorporation of Sn into the ferromagnetic-rich amorphous phase in spite of a rather low melting point of Sn as compared to Fe or Co ones. Furthermore, Sn is an abundant and inexpensive alloying element [2,3,8-10]. In this study the results of the structural and thermodynamic investigation of rapidly quenched  $(\text{Fe/Co})_{85-x}\text{Sn}_x\text{B}_{15}$  systems, for the ratio Fe/Co= 1/0, 0/1 and 1/1 and for Sn  $x= 3.5, 5$  at. % are presented. The alloying of ferromagnetic systems based on Fe-Sn-B, Co-Sn-B and Fe-Co-Sn-B improves the properties of resulting structure composed of the ferromagnetic grains in the amorphous matrix. The samples in nanocrystalline state due to their interesting magnetic properties that are caused by the homogeneous and ultrafine structure. The structure evolution from amorphous state into the crystalline one was observed by the calorimetric (DSC) and thermogravimetric (TGA) measurements. The formation of ferromagnetic grains from the amorphous matrix is shown by the direct structure observation using transmission electron microscopy as well as by the X-ray diffraction methods. The results of in-situ phase analysis at a pre-defined temperature regime are reviewed, too.

### References

- [1] A. Makino, et al., Journal of Applied Physics 91 (2002) 8420.
- [2] Y. Yoshizawa, et al., Mat. Sci. Engn. A 375-357 (2007),207.
- [3] P. Svec, et al., Adv. in Intelligent Systems and Computing 317 (2015) 381.
- [4] I. Janotova, et al., Journal of Electrical Engineering 66 (2015) 297–300.
- [5] K. Suzuki, et al., J. Appl. Phys. 70 (1991) 6232.
- [6] M. Ohta, Y. Yoshizawa, J. Magn. Magn. Mater. 320 (2008) 750.
- [7] P. Svec et al., IEEE Trans. Magn. 46 (2010) 408.
- [8] P. Sharma, X. Zhang, Y. Zhang, A. Makino, Scripta Mater. 95 (2015) 3.
- [9] E. Illekova et al., J. of Alloys and Compounds 509 (2011) S46.
- [10] I. Matkoet al., J. of Alloys and Compounds 615 (2015) S462.

Support of the project APVV-460-12 is acknowledged.

# Theoretical study of electronic structure and electron-phonon coupling in Ta-Ni-Hf-Zr-Ti high entropy alloy

K. Jasiewicz, B. Wiendlocha, P. Korbeń, S. Kaprzyk, J. Tobola

*AGH University of Science and Technology, Al. Mickiewicza 30, 30-059 Krakow, Poland*

High degree of chemical disorder occurring in high entropy alloys (HEA), sometimes regarded as “metallic glasses on ordered crystal lattice” [1], makes the theoretical investigations of their physical properties quite challenging. The Green function Korringa-Korringa-Kohn method combined with the coherent potential approximation (KKR-CPA) [2-4] seems to be particularly well adapted technique to study such materials, since it allows to perform first principles calculations of electronic structure and related quantities (eg. magnetic moments or superconducting parameters) in systems including chemical disorder, in self-consistent way. In this approach the random or quasi-random distribution of constituent elements commonly observed in real HEA systems is replaced by ordered lattice of “CPA medium”, actually representing an average over all possible configurations of the disordered lattice (within the simple unit cell: bcc, fcc or hcp). Quite recently [5], it has been showed that the KKR-CPA calculations applied to investigate crystal stability and magnetic properties of FeCrNiCoAl<sub>x</sub> HEA gave the results consistent with experimental data.

In this work, we present results of the KKR-CPA calculations [6] of the recently discovered first superconducting HEA Ta<sub>34</sub>Nb<sub>33</sub>Hf<sub>8</sub>Zr<sub>14</sub>Ti<sub>11</sub> exhibiting T<sub>c</sub> = 7.3 K [1]. Our calculations show that the Fermi level is located in the large peak of total density of states (DOS) as well as high l-decomposed DOS values on constituent atoms are present, which well support superconductivity appearance in particular compositions of TNHZT-HEA. Since experimental results rather indicate the BCS-type superconductivity, estimations of electron-phonon coupling constant was then attempted. Electronic part of  $\lambda$  [7] has been calculated using the Gaspari–Gyorffy formula within the rigid muffin-tin approximation (RMTA) [8,9], while the phonon part has been approximated using average atomic mass and experimental value of the Debye temperature. Finally, it resulted in the electron-phonon constant ( $\lambda=1.16$ ), which is in close agreement with the value determined from specific heat measurements ( $\lambda=0.98$ ). On the whole, it suggests rather strong electron-phonon coupling in this material. Similiar theoretical analysis was also performed for different compositions of TNHZT-HEA.

- [1] P. Kozelj, S. Vrtnik, A. Jelen, S. Jazbec, Z. Jaglicic, S. Maiti, M. Feuerbacher, W. Steurer, J. Dolinsek, Phys. Rev. Lett. 113, 107001 (2014)
- [2] T. Stopa, S. Kaprzyk, J. Tobola, J. Phys: Condens. Matter 16, 4921 (2004)
- [3] S. Kaprzyk, A. Bansil, Phys. Rev. B 42, 7358 (1990)
- [4] A. Bansil, S. Kaprzyk, P. E. Mijnarends, J. Tobola, Phys. Rev. B 60, 13396 (1999)
- [5] K. Jasiewicz, J. Cieslak, S. Kaprzyk, J. Tobola, J. Alloys Compd. 648, 307 (2015)
- [6] K. Jasiewicz, B. Wiendlocha, P. Korbeń, S. Kaprzyk, J. Tobola, Phys.Stat.Sol. B RRL 10, 415 (2016)
- [7] W. L. McMillan, Phys. Rev. 167, 331 (1968)
- [8] G. D. Gaspari, B. L. Gyorffy, Phys Rev Lett 28, 801(1972)
- [9] W. E. Pickett, Phys. Rev. B 25, 745 (1982)

## Towards the formation of the Al<sub>9</sub>Ir<sub>2</sub> phase as surface compound

Joris KADOK<sup>1</sup>, Katariina PUSSI<sup>2</sup>, Emilie GAUDRY<sup>1</sup>, Marie-Cécile de WEERD<sup>1</sup>, Yurii PROTS<sup>3</sup>, Vincent FOURNEE<sup>1</sup> and Julian LEDIEU<sup>1</sup>

<sup>1</sup>*Institut Jean Lamour UMR7198 CNRS, Université de Lorraine, Parc de Saurupt, 54011, Nancy, France*

<sup>2</sup>*Department of Mathematics and Physics, Lappeenranta University of Technology, P.O. Box 20 FIN-53851 Lappeenranta, Finland*

<sup>3</sup>*Max-Planck-Institut für Chemische Physik fester Stoffe, Nöthnitzer Strasse 40, 01187 Dresden, Germany*

The structural complexity often inherent to Al-based intermetallic compounds can lead to unique chemical and physical surface properties [1]. This has been well demonstrated in the field of heterogeneous catalysis using Al-Cu-Fe quasicrystal [2] and Al<sub>13</sub>TM<sub>4</sub> compounds [3-4]. To understand at a fundamental level the origin of such properties, a detailed knowledge of the surface structure is often required. To this end, one approach consists of studying selected surfaces of centimeter-size single crystal under ultra high vacuum [5]. For the Al-Ir system where several complex metallic alloys have been identified, an alternative route has been chosen due to difficulties inherent to the phase diagram and to the cost of the Ir element.

Here, we report the adsorption of Ir adatoms on the clean Al(100) surface using low energy electron diffraction (LEED), dynamical LEED analysis (LEED I(V)), scanning tunnelling microscopy (STM), x-ray photoelectron spectroscopy combined with *ab initio* calculations. At 300 K, the deposition results in a disordered layer. Between 600 K and 700 K, the LEED patterns consist of two domains interpreted as a ( $\sqrt{5}\times\sqrt{5}$ )R26.6° phase. The dimensions on the domains match with the unit cell parameters of the Al<sub>9</sub>Ir<sub>2</sub> compound. The orientation of the Al<sub>9</sub>Ir<sub>2</sub> domains with respect to the Al(100) surface is dictated by the alignment of the Al square motifs present in Al<sub>9</sub>Ir<sub>2</sub> layers with the square surface unit mesh of Al(100). The topmost surface layer of the Al<sub>9</sub>Ir<sub>2</sub> phase formed is Al terminated as demonstrated by *ab initio* calculations. Indeed, the calculated segregation of Ir in Al(100) shows a preferential positioning of Ir atom in the subsurface layers. On top of these Al<sub>9</sub>Ir<sub>2</sub> domains, STM measurements reveal the presence of overlayers referred as a (2x2) reconstruction of the ( $\sqrt{5}\times\sqrt{5}$ )R26.6° phase and a “14.3 Å” structure. The latter can be associated with an incomplete Al layer present in the Al<sub>9</sub>Ir<sub>2</sub> compound. A thorough LEED I(V) analysis points toward the simultaneous presence of Ir adatoms in the subsurface layer of Al(100) and the presence of Al<sub>9</sub>Ir<sub>2</sub> domains. In other words, the different stages towards the growth of the Al<sub>9</sub>Ir<sub>2</sub> compound coexist under our dosing conditions.

[1] J.-M. Dubois, Chem. Soc. Rev. 41, (2012) 6760.

[2] T. Tanabe, S. Kameoka, and A. P. Tsai, Appl. Catal. A384, (2010) 241.

[3] M. Armbrüster, K. Kovnir, M. Friedrich, *et al.* Nat. Mater. 11, (2012) 690.

[4] J. Ledieu, E. Gaudry, L.N. Serkovic, *et al.* Phys. Rev. Lett. 110, (2013) 076102.

[5] J. Ledieu, E. Gaudry, and V. Fournée, Sci. Technol. Adv. Mater. 15, (2014) 034802.

# Single crystal growth of Sb-based thermoelectric materials by *Inclined Rotary Bridgman* method

Mirtha Pillaca<sup>1</sup>, Oliver Harder<sup>1</sup>, Wolfram Miller<sup>2</sup>, Peter Gille<sup>1</sup>

<sup>1</sup>Ludwig-Maximilians-Universität München, 80333 München, Germany

<sup>2</sup>Leibniz Institute for Crystal Growth (IKZ), 12489 Berlin, Germany

Many binary intermetallic compounds cannot be crystallized from congruent melts but have to be grown below their specific peritectic temperature  $T_p$ . FeSb<sub>2</sub> ( $T_p = 750^\circ\text{C}$  [1]) and CoSb<sub>3</sub> ( $T_p = 874^\circ\text{C}$  [2]) and third-component modifications based on these structures are considered to be interesting materials for thermoelectric applications [3]. They can only be crystallized from Sb-rich solutions containing more than 90 at. % Sb. Moreover, due to the relatively high Sb vapor pressure, crystal growth has to be carried out in closed ampoules, e.g. using the Bridgman method from a high-temperature solution. In vertical Bridgman experiments buoyancy-driven convection is too slow to completely remove the excess component (Sb) from the growing interface. Strong mixing that is mandatory in high-temperature solution growth can be achieved by rotating the ampoule that is tilted (together with the Bridgman-type tube furnace) with respect to the axis of gravity. Three-dimensional calculations of the melt convection by employing the commercial software package ANSYS-cfx show the remarkable increase in melt flow under *Inclined Rotary Bridgman* conditions achieved for a tilting angle of  $75^\circ$ . The marker distribution pattern indicates an efficient transport all along the interface. The very effective forced convection by inclined rotation of the ampoule could also be visualized in model experiments studying the dissolution rate of colored single crystals (CuSO<sub>4</sub>·5H<sub>2</sub>O) by time-resolved optical spectroscopy. Inclusion-free FeSb<sub>2</sub> and CoSb<sub>3</sub> crystals could be obtained from *Inclined Rotary Bridgman* experiments using an ampoule rotation rate of 100 rpm and a pulling rate of 0.1 mm/h. Experiments using spontaneous nucleation suffer from the high supercooling that occurs in these systems which always results in a sudden crystallization of a huge number of small grains. For single crystal growth, therefore, native seeding is necessary and resulted in first single crystalline ingots with 15 mm diameter and about 20 mm in length.

It is worth mentioning that the advantage of this *Inclined Rotary Bridgman* method is not at all restricted to the Sb-based thermoelectric materials but may be a powerful approach in unidirectional solidification from off-stoichiometric melts, in general.

[1] K.W. Richter, H. Ipsen, J. Alloys Comp. **247**, 247 (1997).

[2] H. Okamoto, J. Phase Equil. **12**, 244 (1991).

[3] M. Rull-Bravo, A. Moure, J.F. Fernández, M. Martin-González, RSC Adv. **5**, 41653 (2015).

## Study of phase equilibria in Ga-Co-Cu system at 830°C

<sup>1</sup>Pavol Priputen, <sup>1</sup>Marián Drienovský, <sup>1</sup>Ivona Černičková, <sup>2</sup>Jozef Janovec

<sup>1</sup>*Slovak University of Technology in Bratislava, Faculty of Materials Science and Technology in Trnava, J. Bottu 25, 917 24 Trnava, Slovakia*

<sup>2</sup>*Slovak University of Technology in Bratislava, Vazovova 5, 812 43 Bratislava, Slovakia*

Ternary system Ga-Co-Cu belongs to rarely studied systems in terms of phase equilibria. According to Ge & Kuo [1] both icosahedral and decagonal quasicrystals are present in several Ga-Co-Cu alloys after annealing at 830°C. However, there was not published any isothermal section of the Ga-Co-Cu phase diagram, till now. To fill this gap, a more detailed experimental examination of phase equilibria in Ga-Co-Cu system at 830°C was done. For this purpose, series of alloys were prepared, annealed at 830°C for 330 h and subsequently rapidly cooled to preserve their as-annealed microstructure. The obtained samples were further studied by scanning electron microscopy, energy-dispersive x-ray spectroscopy and x-ray diffraction. As a result, isothermal section at 830°C was proposed.

[1] S.P. Ge and K. H. Kuo, Icosahedral and stable decagonal quasicrystals in  $\text{Ga}_{46}\text{Fe}_{23}\text{Cu}_{23}\text{Si}_8$ ,  $\text{Ga}_{50}\text{Co}_{25}\text{Cu}_{25}$  and  $\text{Ga}_{46}\text{V}_{23}\text{Ni}_{23}\text{Si}_8$ , *Philos. Mag. Lett.* **75** (1997), pp. 245-253.

### Acknowledgements

The authors wish to thank to the European Regional Development Fund (ERDF) for financial support of the project ITMS:26220120048 “Center for development and application of advanced diagnostic methods in processing of metallic and non-metallic materials” funded within the Research & Development Operational Programme, to the Grant Agency VEGA for the financial support under contract 1/0018/15 and to the Slovak Research and Development Agency for the financial support under contracts APVV-0076-11 and APVV-15-0049.

## Improving glass-forming ability of CoFeBSiNb alloys

<sup>1</sup>V. Sidorov, <sup>2</sup>P. Svec

<sup>1</sup> *Ural State Pedagogical University, Ekaterinburg, Russia*

<sup>2</sup> *Institute of Physics SAS, Bratislava, Slovakia*

The influence of Ga, Zr, Sn and Sb small additions on glass forming ability (GFA) of CoFeNbBSi metallic alloys with different compositions of the base elements has been investigated. The bulk metallic glasses in the form of rods with diameter of 1 - 4 mm were prepared by the cast suction method and by melt injection into water cooled copper mold. The research has been carried out by means of X-ray diffraction, TEM and DSC studies, as well as electrical resistivity and magnetic susceptibility measurements in crystal and liquid states. The additions of Ga and Zr were found to improve glass forming ability of the alloys, whereas Sn and Sb additions decrease it. However, the existing criteria of GFA cannot explain such an influence; it is necessary to introduce a new one, containing information about the melt before quenching. For example, the paramagnetic Curie temperature in the melt is able to describe quantitatively the influence of the additions: in case the addition increases it, the GFA improves.

The work is partially supported by the Ministry of Education and Science of the Russian Federation (Project no. 4.1177.2014/K).

## Electronic structure and properties of $(\text{TiZrNbCu})_{1-x}\text{Ni}_x$ high entropy amorphous alloys

<sup>1</sup>Katica Biljaković, <sup>2</sup>György Remenyi, <sup>3</sup>Ignacio A. Figueroa, <sup>4</sup>Ramir Ristić, <sup>5</sup>Damir Pajić, <sup>6</sup>Ahmed Kuršumović, <sup>1</sup>Damir Starešinić, <sup>5</sup>Krešo Zadro and <sup>5</sup>Emil Babić

<sup>1</sup>*Institute of Physics, Zagreb, Croatia*

<sup>1</sup>*Institut Neel, Universite Grenoble Alpes, Grenoble, France*

<sup>1</sup>*Institute for Materials Research-UNAM, Ciudad Universitaria Coyoacan, Mexico D.F., Mexico*

<sup>1</sup>*Department of Physics, University of Osijek, Osijek, Croatia*

<sup>1</sup>*Department of Physics, Faculty of Science, Zagreb, Croatia*

<sup>2</sup>*Department of Materials Science & Metallurgy, University of Cambridge, , Cambridge, UK*

Comprehensive study of the low temperature specific heat (LTSH), magnetic susceptibility  $\chi_{\text{exp}}$  and the Young's modulus (E) of  $(\text{TiZrNbCu})_{1-x}\text{Ni}_x$  amorphous high entropy alloys (a-HEA) [1] has been performed. LTSH revealed that the electronic density of states at the Fermi level,  $N(E_F)$ , decreases with increasing x, whereas the Debye temperature ( $T_D$ ) increases with x. This is similar to what is observed in glassy alloys of early transition (TE) metals with late transition (TL) metals [2] and indicates that  $N(E_F)$  is dominated by d-electrons of TE. E increases with x showing enhanced interatomic bonding. The applicability of the rule of mixture (RoM) to these and other HEA is briefly discussed.

[1] A. Cunliffe, J. Plummer, I. Figueroa and I. Todd, *Intermetallics* **23**, 204 (2012).

[2] R. Ristić, J. R. Cooper, K. Zadro, D. Pajić, J. Ivkov and E. Babić, *J. Alloys Compd.* **621**, 136 (2015).and references therein

## **Formation of monophasic Fe<sub>23</sub>B<sub>6</sub>-type alloy via crystallization of amorphous Fe-Ni-Nb-B system**

Peter Svec, Peter Svec Sr., Jozef Hosko, Dusan Janickovic

*Institute of Physics, Slovak Academy of Sciences, Bratislava, Slovakia*

...

This study is focused on rapidly quenched Fe-Ni-Nb-B system in a wide compositional range of substitution of Fe by Ni with varying boron content. This system is known to have a good glass forming ability ( $\Delta T_x$  up to 49K at 40K/min) and to crystallize in either two distinct transformation stages or in one single step, depending on the boron content and on the ratio of Fe to Ni. On the basis of our results we have identified and quantified the formation of a complex phase (Fe-Ni-Nb)<sub>23</sub>B<sub>6</sub> alongside with fcc-FeNi. In a specific case it was possible to obtain only a single-phase Fe<sub>23</sub>B<sub>6</sub> type alloy and thus allowing to explore and characterize this phase, especially as there is no prior evidence of preparing such a monophasic system. Detailed characterization of composition, structure and selected magnetic properties of both phases will be presented. We have proposed a model of possible local structural and chemical arrangement in (Fe-Ni-Nb)<sub>23</sub>B<sub>6</sub> phase as well as possible building units responsible for specific features of transformation from amorphous state and for preferential formation of this phase. This was confirmed by refinement of selected X-ray patterns together with high resolution (S)TEM analysis combined with energy filtered TEM. EFTEM analysis has shown a unique interface between the Fe<sub>23</sub>B<sub>6</sub>-type phase and the remaining FeNi matrix in systems where both phases are present. On the other hand, high resolution z-contrast STEM analysis applied to a single phase system revealed atomic positions of constituent atoms. Niobium was confirmed on positions as predicted by the proposed structural model and as refined from the diffraction experiments. Conventional high resolution TEM analysis was used to characterize the Fe<sub>23</sub>B<sub>6</sub>-type grains with respect to defects and faults.

Support of the project APVV-15-0621 is acknowledged.

## Structure And Properties of Soft-Magnetic Amorphous Bilayer Ribbons

P. Švec<sup>1</sup>, I. Mařko<sup>1</sup>, J. Marcin<sup>2</sup>, J. Kováč<sup>2</sup>, G. Vlasák<sup>1</sup>, D. Janičkovič<sup>1</sup>,  
I. Škorvánek<sup>2</sup>, P. Švec Sr.<sup>1</sup>

<sup>1</sup>*Institute of Physics, Slovak Academy of Sciences, Bratislava, Slovakia*

<sup>2</sup>*Institute of Experimental Physics, Slovak Academy of Sciences, Košice, Slovakia*

...

Rapidly quenched bilayers consisting of Fe-Si-B and Co-Si-B layers have been prepared by planar flow casting from a single crucible with two nozzles close to each other and with a partition between them forming two separate vessels. Such an arrangement has allowed to obtain ribbons with two homogeneous layers, one on top of the other, along the whole ribbon length with high quality surface and with contact interlayer having submicron thickness. Ribbons with typical thickness of 45-50 microns and 6 mm width exhibited amorphous structure of both layers in as-quenched state. Temperature dependencies of electrical resistivity, dilatation and magnetization have been investigated in the amorphous state and during crystallization of both layers, which take place at different temperatures.

The structure of the interlayer has been investigated by cross-sectional TEM, XRD, SEM/EDX. From the results it seems evident that the process of connection of the two layers during preparation takes place by solidification with only a small extent of mutual interdiffusion of component atoms localized to a narrow well-defined interface, leading to mechanically solid connection between the two layers. The effect of combined presence of two different soft magnetic alloys on the overall magnetic properties is presented with respect to potential applications of such materials.

Support of the project APVV-460-12 is acknowledged.

# Phase transformations up to melting point in Al-(Fe, Co, Ni)-Si alloys

<sup>1</sup>Juraj Zigo, <sup>2</sup>Oleksandr Roik, <sup>1</sup>Peter Švec

<sup>1</sup>Institute of Physics, Slovak Academy of Sciences, Bratislava, Slovakia

<sup>2</sup>TarasShevchenko National University of Kyiv, Kyiv, Ukraine

Rapidly quenched Al-T-Si alloys (where T stands for transition metal) have high potential as light-weight yet high-strength construction materials. For potential applications, it is crucial to have detailed knowledge of phase composition upon heat treatment. Evolution of structure during heating from room temperature up to 500°C was investigated before [1]. In our study, we focused on properties of Al based alloys containing as much as 20 at. % of Si. To achieve amorphous structure after rapid quenching, we used 10-15 at. % of transition metal (namely Fe, Co and Ni).

In recent study, evolution of structure during heating up to melting point and on subsequent solidification during cooling is investigated. For this purpose, high-temperature (up to 925°C) in-situ X-ray diffraction (Mo K $\alpha$ ) was used. Temperatures of XRD measurements were selected in accordance to temperatures of phase transformations obtained by differential thermal analysis (DTA) (Fig. 1a).

In Al-Ni-Si system with composition of Al<sub>65</sub>Ni<sub>15</sub>Si<sub>20</sub> after annealing from initially amorphous state to 245°C, unknown hexagonal ternary phase appeared. To determine structure of this phase, further investigation is needed. In-situ XRD measurements at temperatures from ~500°C up to melting reveals several solid state phase transformations and meltings of multiple phases. Similar investigation was performed for other alloys (namely Al<sub>70</sub>Ni<sub>10</sub>Si<sub>20</sub>, Al<sub>70</sub>Co<sub>10</sub>Si<sub>20</sub>, Al<sub>65</sub>Fe<sub>15</sub>Si<sub>20</sub>). Obtained structure data is mainly in accordance with phase diagrams [2]–[4]. However in-situ XRD shows some unidentified peaks.

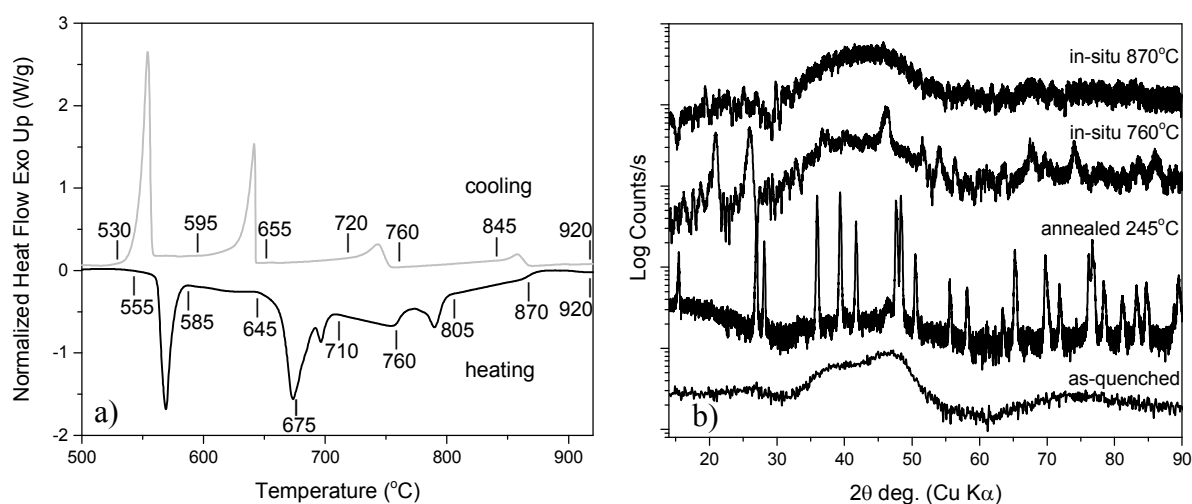


Fig 1: a) DTA data showing several phase transitions in Al<sub>65</sub>Ni<sub>15</sub>Si<sub>20</sub> upon heating (bottom line) and cooling (upper line). Indicated are temperatures of in-situ XRD measurements. b) XRD of Al<sub>65</sub>Ni<sub>15</sub>Si<sub>20</sub> in as-cast state, annealed and at non-ambient temperatures.

- [1] J. Zigo et al., “Evolution of Complex Phases in Al-Fe-Si Systems,” *Mater. Res.*, vol. 18, pp. 141–145, Nov. 2015.
- [2] V. Raghavan, “Al-Fe-Si” *J. Phase Equilibria Diffus.*, vol. 30, no. 2, pp. 184–188, 2009.
- [3] V. Raghavan, “Al-Co-Si” *J. Phase Equilibria Diffus.*, vol. 29, no. 1, pp. 57–59, 2008.
- [4] O. Fabrichnaya et al., “Aluminium – Nickel – Silicon,” in *Landolt-Boernstein. Num. Data and Func. Relationships in Sci. and Tech. (New Series)*, 2004, pp. 400–424.

Support of the project APVV-15-0738 is acknowledged.



**Marc de Boissieu (Editor)**  
**Marek Mihalkovic (Editor)**  
**Peter Svec (Editor)**

## **C-MAC Days 2016**

### **Program and Abstracts**

Published and printed by  
VEDA, Publishing House of the Slovak Academy of Sciences  
Dúbravská cesta 9  
845 02 Bratislava  
Slovakia  
<http://www.veda.sav.sk>

ISBN 978-80-224-1540-8

Edition No. 4223

Bratislava 2016



Monday November 21		Tuesday November 22		Wednesday November 23		Thursday November 24	
		9.00-9.30	Dolinsek	9.00-9.30	Mace	9.00-10.30	GB+SB meet.
		9.30-9.50	Cieslak	9.30-9.50	Tobola	10.30-11.00	<b>Coffee break</b>
		9.50-10.10	Vrtnik	9.50-10.10	Popcevic	11.00-12.30	Gen.Assembly
		10.10-10.30	Plevachuk	10.10-10.30	Synoradzki	12.30-14.00	<b>Lunch</b>
		10.30-11.00	<b>Coffee break</b>	10.30-11.00	<b>Coffee break</b>		
		11.00-11.30	Kozelj	11.00-11.30	Widmer		
		11.30-11.50	Jelen	11.30-11.50	Sidorov		
		11.50-12.10	Gille	11.50-12.10	Pavlosiuk		
		12.10-12.30	Minelli	12.10-12.30	Grin		
		12.30-14.00	<b>Lunch</b>	12.30-14.00	<b>Lunch</b>		
		14.00-14.30	Ben-Abraham	14.00-14.30	Tomes		
		14.30-14.50	Buganski	14.30-14.50	Anand		
		14.50-15.10	Kurihara	14.50-15.10	de Boissieu		
		15.10-15.30	Mihalkovic	15.10-15.40	<b>Coffee break</b>		
		15.30-16.00	<b>Coffee break</b>	15.40-16.00	Stolz		
16.00-20.00	<b>Registration</b>	16.00-16.30	Aviziotis	16.00-16.20	Wencka		
		16.30-16.50	Gaudry	16.20-16.40	Coates		
		16.50-17.10	Janovec	16.40-17.00	Krajci		
		17.10-17.30	Roik				
19.00-22.00	<b>Welcome reception</b>	17.30-19.00	<b>Poster Session</b>				
		19.00-21.00	<b>Dinner</b>	18.30-24.00	<b>Gala Dinner</b>		